Research article

The protective effects of selenium and boron on cyclophosphamide-induced hepatic oxidative stress, inflammation, and apoptosis in rats

Mustafa Cengiz [a,*], Bahri Gür [b,**], Fatma Gür [c], Varol Şahintürk [d],
Alpaslan Bayrakdar [e], Ilknur Kulcanay Şahin [f], Sıla Appak Başkoy [g], Namık Bilici [h],
Suzan Onur [i], Yağmur Kaya [j], İsa Kıran [j], Özge Yıldırım [j], Nur Banu Akkaya [j],
Canan Vejselova Sezer [k], Adnan Ayhanci [j]

[a] Department of Elementary Education, Faculty of Education, Siirt University, Siirt, Turkiye
[b] Department of Biochemistry, Faculty of Sciences and Arts, Iğdır University, Iğdır, Turkiye
[c] Department of Dentistry Services, Atatürk University, Erzurum, Turkiye
[d] Department of Histology and Embryology, Medical Faculty, Eskisehir Osmangazi University, Eskişehir, Turkiye
[e] Vocational School of Healthcare Services, Iğdır University, Iğdır, Turkiye
[f] Vocational School of Health Services, Kırıkkale University, Kırıkkale, Turkiye
[g] Faculty of Science, Ryerson University, Toronto, Ontario, Canada
[h] Department of Medical Pharmacology, Faculty of Medicine, Karabük University, Karabük, Turkiye
[i] Faculty of Health Sciences, Karabük University, Karabük, Turkiye
[j] Department of Biology, Faculty of Science, Eskişehir Osmangazi University, Eskişehir, Turkiye
[k] Department of Biology, Faculty of Science, Eskişehir Technical University, Eskişehir, Turkiye

ARTICLE INFO

ABSTRACT

Cyclophosphamide (CP) is an alkylating anticancer drug with broad clinical application that is highly effective in the treatment of cancer and non-malignant diseases. However, the main limiting effect of CP is multi-organ toxicity due to damage to normal tissues. The aim of this study is to compare the hepatoprotective potential of selenium (Se) and boron (B) in CP-induced liver injury in experimental rats. The rats were randomly divided into six equal groups: Control (saline), 200 mg/kg CP (administered once on the fourth day of the experiment), 1.5 mg/kg Se (administered once/time daily for 6 days), 20 mg/kg B (administered once/time daily for 6 days), Se + CP and B + CP administered intraperitoneally (i.p.). Administration of CP leads to an increase in the levels of apoptotic markers (Bax, caspase-3), the apoptotic signaling pathway (Nrf2), oxidative stress indicators (TOS, OSI), lipid peroxidation markers (MPO, MDA), inflammation levels (NF-kB, TNF-α, IL-1β, IL -6), liver function markers (ALT, AST, ALP), while apoptosis markers (Bcl-2), apoptosis pathway (Keap-1), oxidative stress indicator (TAS), inflammation (IL -10) and intracellular antioxidant defense system (SOD, CAT, GPx and GSH) decreased. In addition, degeneration of hepatocytes and congestion in the central veins were observed. In contrast, in the groups administered Se and B with CP, the changes that occurred were reversed. However, it was found that Se protects the liver slightly better against CP damage than B. The protective effect of Se and B against the toxic effects of CP on the antioxidant markers SOD, CAT

and GPx1 was also investigated *in silico*. The *in silico* results were consistent with the *in vivo* results for SOD and CAT, but not for GPx1.

Abbreviation list

CP	Cyclophosphamide
B	Boron
ACR	Acrolein
FAM	Phosphoramide mustard
AO	Antioxidant defense system
Se	Selenium
SOD	Superoxide dismutase
CAT	Catalase
GPx1	Glutathione peroxidase-1
H&E	Hematoxylin-eosin
AST	Aspartate Aminotransferase
ALP	Alkaline phosphatase
ALT	Alanine aminotransferase
MPO	Myeloperoxidase
MDA	Malondialdehit
GSH	Glutathione
TOS	Total Oxidant Status
TAS	Total Antioxidant Status
OSI	Oxidative Stress Index
ELISA	Enzyme-linked immunosorbent assay
NF-kB	Nuclear factor kappa B
TNF-α	Tumor necrosis factor-α
IL -6	Interleukin-6
IL -1β	Interleukin-1β
IL-10	Interleukin-10

1. Introduction

Cyclophosphamide CP) is an alkylating chemotherapeutic agent with broad clinical application that has been shown to be effective in the treatment of cancer and non-malignant diseases. The antitumor efficacy of CP depends on its ability to be used at high doses. The main limiting effect of CP is multi-organ toxicity [1–3]. These dose-limiting toxicities are hematotoxicity, urotoxicity, nephrotoxicity, hepatotoxicity, cardiotoxicity and myelotoxicity [4–7]. Among these, nephrotoxicity and hepatotoxicity are considered the two most important side effects, as the kidney and liver are important organs responsible for the metabolism and excretion of CP and its reactive metabolites [8]. CP is metabolically activated by hepatic enzymes and forms 4-hydroxy-CP, which is converted into two toxic metabolites: Phosphoramide mustard (FAM) and acrolein (ACR) [9]. These reactive metabolites lead to oxidative stress and cause oxidative damage to cellular macromolecules such as nucleic acids, proteins and lipids [10]. The antineoplastic properties of CP are associated with FAM. It is assumed that FAM inhibits cell division by binding to DNA and mediates the immunosuppressive and antitumor effects of CP [6,11–13]. The toxic effects of CP are related to its active metabolite ACR. ACR disrupts the tissue antioxidant defense system (AO), leading to a high rate of reactive oxygen species (ROS) formation and is mutagenic to mammalian cells. The ACR-derived ROS bind to molecules such as enzymes, receptors and ion pumps and disrupt their functions [11]. To avoid these toxic effects of ACR in neoplastic diseases, detoxification using some AO agents should be performed during CP chemotherapy. Recent studies have also shown that AO suppresses the initiation and development of carcinogenesis and prevents cell death and alterations [12]. Some *in vivo* and *in vitro* results suggest that cellular toxicities caused by cytotoxic agents can be significantly prevented by the use of certain trace elements such as Se and B [6,13]. However, there are very few studies in the literature comparing the efficacy of Se and B in the prevention of CP-induced liver injury.

Se is a trace element that protects cells from oxidative stress and plays a key role in the AO mechanism, and it is claimed that this property allows it to have a protective effect on tissue damage. Significant liver changes have also been observed in rats with Se deficiency [14,15]. On the other hand, there are also studies that show Se deficiency in liver cirrhosis [16]. Animal studies have shown that Se can reduce liver fibrosis [17,18]. Se has been shown to protect against some cancers, increase male fertility, reduce cardiovascular mortality and suppress the production of inflammatory mediators in asthma [19,20].

B is a trace element that has been reported to have a synergistic effect with chemotherapeutic agents, increasing the therapeutic

Table 1
Group classification, administration dose and treatment schedule.

Number	Group (n = 6)	Dose, route, and duration
1.	Control	0.5 mL saline, i.p. once a day for 6 days and sacrificed on the 7th day
2.	Se	1.5 mg/kg, i.p. once a day for 6 days and sacrificed on the 7th day [27]
3.	B	20 mg/kg, i.p. once a day for 6 days and sacrificed on the 7th day [28]
4.	CP (Toxic)	200 mg/kg, i.p. once on the 4th day and sacrificed on the 7th day [23]
5	Se + CP	1.5 mg/kg, i.p. once a day for 6 days +200 mg/kg, i.p. once on 4th day and sacrificed on 7th day
6	B + CP	20 mg/kg, i.p. once a day for 6 days +200 mg/kg, i.p. once on 4th day and sacrificed on 7th day

Se: Selenium, B: Boron, CP: Cyclophosphamide.

efficacy of antineoplastic drugs and reducing the toxic side effects of cytotoxic agents such as cisplatin thanks to its interaction with AOs as well as its protective function for the cell membrane by inhibiting lipid peroxidation [13,21]. This is explained by the fact that B inactivates the ROS and thus prevents the formation of lipid peroxidation [22].

Against this background, this study aims to determine whether Se and B can effectively prevent CP-induced liver injury by modulating intracellular antioxidant status, apoptosis and inflammation. In addition, this study aims to investigate the potential effects of Se and B on superoxide dismutase (SOD), catalase (CAT) and glutathione peroxidase-1 (GPx1), one of the elements of the intra-cellular antioxidant system, both *in vivo* and for the first time through *in silico* studies.

2. Material and methods

2.1. Animal treatment

The boron compound, 99 % pure boric acid, was purchased commercially, and Se (seleno-L-methionine, S3132) and CP were obtained from Sigma (Germany). Of these substances, 500 mg of CP was dissolved in 25 mL of physiological saline and prepared for injection [23]. The chemical injections were administered intraperitoneally (i.p.) with sterile disposable syringes after the solutions had been freshly prepared. The solution was prepared by dissolving 1.5 mg/kg Se [24] and 20 mg/kg B [25,26] in 0.5 mL saline and administered i.p. All animals were weighed and the drug doses to be administered were determined. The weight of the animals was determined before the first injection and sacrifice. The doses and duration of chemical administration to all experimental groups are shown in Table 1.

For the experiment, male Sprague-Dawley rats weighing 200–250 g were selected and randomly divided into six groups: Control, CP, B, Se, B + CP, and Se + CP. For six days, the rats in this study received intraperitoneal (i.p.) injections of 1.5 mg/kg Se and 20 mg/kg B. Only on the fourth day of the experiment was a single dose of CP (200 mg/kg) injected intraperitoneally. Blood and liver samples were taken while the rats were sedated.

2.2. Anesthesia and surgical applications

All experimental studies were performed with hygienic surgical equipment. Intracardiac blood sampling was performed in animals anesthetized with ketamine (50 mg/kg)/xylazine (10 mg/kg). Blood samples were centrifuged at 3000 rpm for 10 min and serum were collected. The serum samples placed in polyethylene tubes were stored in the freezer at −80 °C for biochemical assays. The livers were collected and weighed. The liver weight index (LWI) were calculated using the following formula.

*LWI = (liver weight/body weight (BW)) × 100.

2.3. Histological examinations

For histopathological examination, the liver specimens were cut into small pieces and fixed in Bouin's solution. After dehydration in ethanol (70, 90, 96, 100 %), the tissue samples were cleaned in xylene, embedded in paraffin, and cut into sections of 5–6 μm. The liver sections were then stained with hematoxylin-eosin (H-E) and Masson's trichrome (Masson).

2.4. Immunohistochemical examinations

Liver tissue samples were regularly deparaffinized and rehydrated before being heated in an oven at 700 W for 10 min and then antigenized with citrate buffer (pH 6.0). After blocking with 3 mL H2O2 and porcine serum, the sections were incubated with primary antibodies against Bax, Bcl-2 and caspase-3. Immunohistochemical analyzes of Nrf2 and Keap-1 were performed according to tech-niques performed in previous studies [26]. Slides were cleared in phosphate-buffered saline and then treated with a secondary anti-rabbit antibody for 45 min. After visualization with a DAB kit, samples were counterstained with Mayer's hematoxylin.
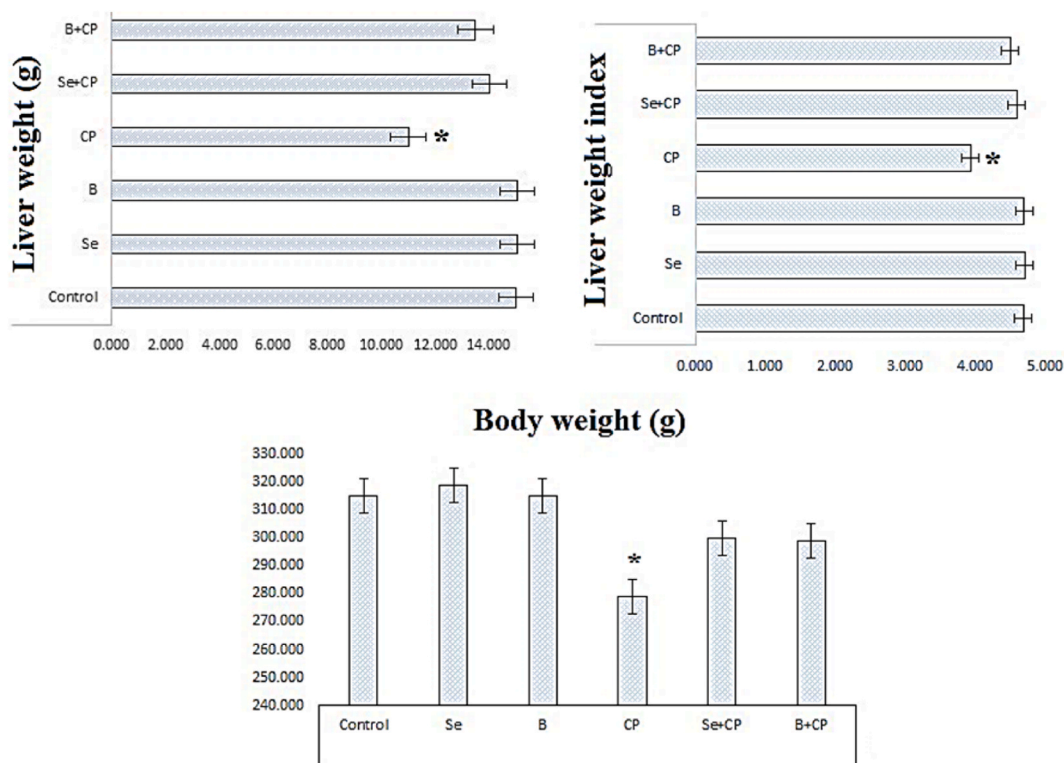
Fig. 1. The body weights, liver weights, and the relative liver weights of rats (mean ± standard deviation). *Significant difference of $p < 0.05$ compared to the control group. Se: Selenium, B: Boron, CP: Cyclophosphamide.

2.5. Measurement of liver function markers

Enzymatic colorimetric methods were used to assess serum levels (aspartate aminotransferase (AST), alkaline phosphatase (ALP), alanine aminotransferase (ALT) [13,29].

2.6. Determination of the values of the antioxidant defense system and lipid peroxidation markers in serum

Serum levels of SOD, CAT, MPO, GPx, MDA, and GSH were measured using a commercially available colorimetric kit.

2.7. Determination of the level of oxidative stress in the serum

TOS and TAS were measured in serum using a commercially available colorimetric assay kit. The OSI value was calculated based on the TOS/TAS ratio [30].

2.8. Identification of proinflammatory cytokines

The proinflammatory cytokines in serum were measured using commercially available ELISA kits (enzyme-linked immunosorbent assay). The concentrations of nuclear factor kappa B (NF-kB), tumor necrosis factor-α (TNF-α), interleukin-6 (IL-6), interleukin-10 and interleukin-1β (IL-1β) were determined using a rat ELISA kit. The analyzes were performed using an ELISA plate reader (Bio-Tek, Winooski, VT, USA).

2.9. Molecular modeling studies

The software package AutoDockTools (1.5.6) was used for molecular docking studies. In this study, the three-dimensional crystal structures of the target proteins CAT (PDB ID: 1TGU), SOD (PDB ID: 1CBJ) and GPx1 (PDB ID: 2F8A) were downloaded from the protein database. Using the AutoDockTools (1.5.6) software, water molecules were first removed from the protein structures prior to molecular docking. Then hydrogen atoms were added and non-polar hydrogen atoms were combined. Finally, the protein structures were prepared by adding Kollman charges. The molecular structure of the Se, B and CP ligand molecules to be used in the molecular docking study was downloaded from the freely accessible PubChem website. The ligands were added to the receptor structures and the
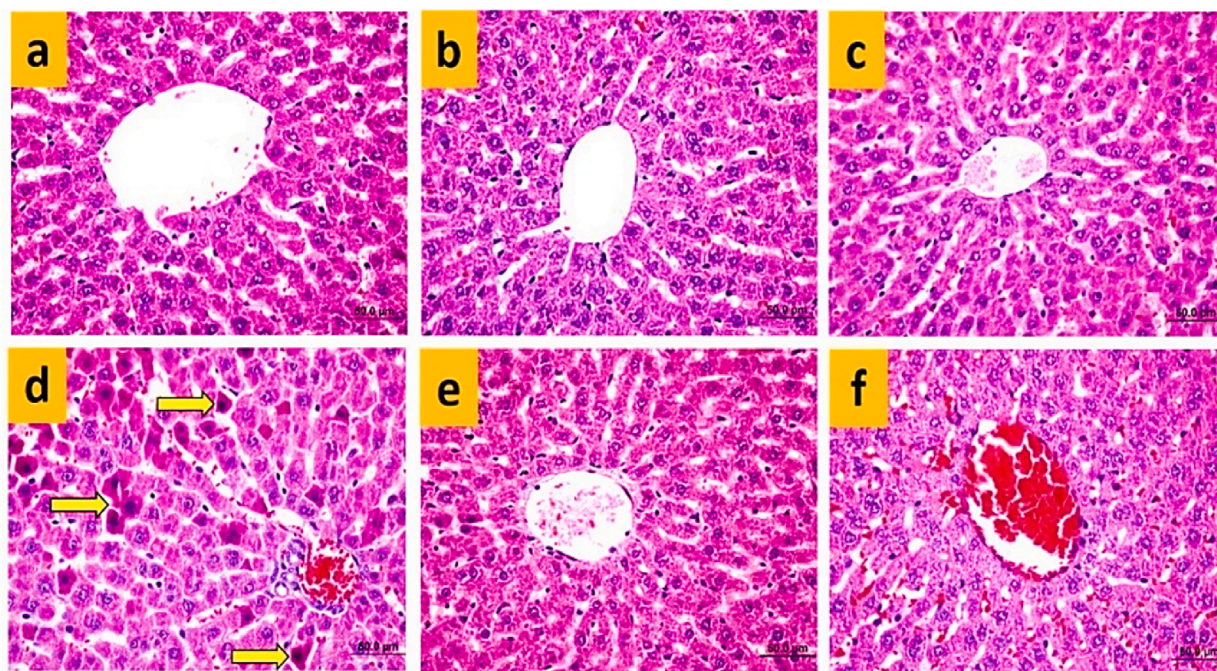
Fig. 2. Microscopic liver images according to experimental groups. Shown are the control group (a), the Se group (b), the B group (c), the CP group (d), the Se + CP group (e) and the B + CP group (f). It can be observed that the control, Se and B groups have a typical histological appearance. In the CP group, the presence of degenerated hepatocytes (yellow arrows) and congestion can be seen. In the B + CP group, the congestion also did not completely regress. However, it can be seen that the Se + CP group has an appearance close to that of the control group. Bar: 50 μm, hematoxylin-eosin.

rotatable bonds were determined for the ligands. After defining a grid box with a grid spacing of 0.375 Å for each protein using AutoGrid4, molecular docking was performed. When performing the docking procedure, the default parameters were selected and Lamarck's genetic algorithm was used to calculate the binding free energy. The complex structure with the lowest binding free energy was selected as the final conformation and the binding free energy was considered as the docking score. In the molecular docking study, the docking procedures were first performed separately between the proteins (SOD, CAT and GPx1) and Se, B and CP. In the second step, the molecular docking study was repeated between the Protein@Se and Protein@B complexes and CP formed in the previous step and the types and lengths of interactions between the proteins and ligands used were visualized and analyzed using the BIOVIA discovery studio program.

2.10. Validation studies

In addition to molecular docking, validation studies of the interactions of the CuZnSOD macromolecule with Se and B were performed considering the specific CuZnSOD activators previously reported in the literature. The activator molecules presented in the literature were selected for CuZnSOD as lactose, maltose, sucrose and trehalose molecules [31].When performing the validation studies, the method from our previous studies was taken into account [12]. In the validation experiments, the binding energy values and root-mean-square deviation (RMSD) values were considered and the techniques established for docking operations were used. The RMSD values are usually calculated only for the moveable heavy atoms with respect to the optimal binding mode. The two RMSD values that AutoDock Vina calculates are the RMSD lower bound and the RMSD upper bound. These variations are based on the way the atoms are matched to determine the distance [32].

2.11. Statistical analyses

Statistical analysis was performed using the programs SPSS 20.0 and Sigma Stat 3.5. Continuous quantitative data; n was expressed as mean and standard deviation, and qualitative data were expressed as n, median, 25th and 75th percentiles. Continuous data that consisted of independent measures and were normally distributed were determined using the one-way ANOVA test (Tukey and Student-Newman-Keuls methods are used in multiple comparisons of this test), and data that consisted of score variables that did not have a normal distribution were analyzed using the Kruskal-Wallis test (Tukey and Student-Newman-Keuls methods are used in multiple comparisons of this test). The differences between the experimental groups that resulted in a numerical value (p) in all statistical applications were considered significant if $p < 0.05$.
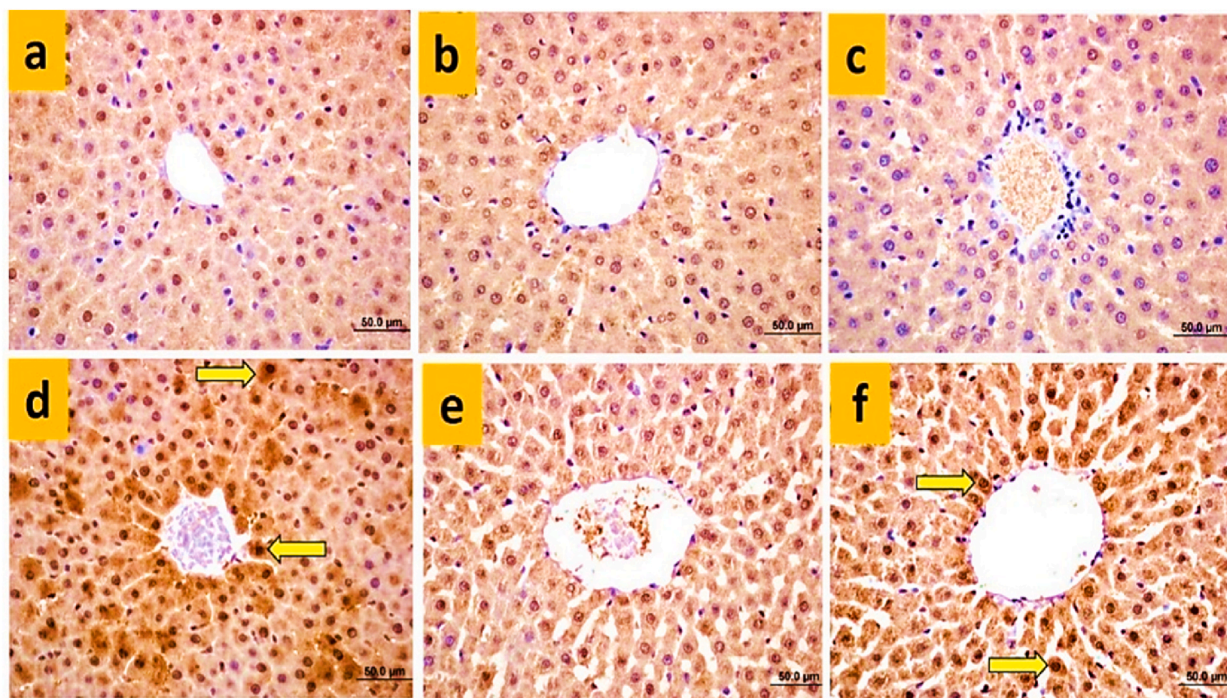
Fig. 3. Microscopic liver images according to experimental groups. Shown are the control group (a), the Se group (b), the B group (c), the CP group (d), the Se + CP group (e) and the B + CP group (f). It can be observed that there is no significant positive staining (apoptosis) in the control, Se, and B groups. In the CP group, positive staining of apoptotic hepatocytes (yellow arrows) is conspicuous. Although the number of apoptotic cells (yellow arrows) decreased in the B + CP group, they still appear to be present. However, it can be observed that the number of apoptotic cells is significantly reduced in the Se + CP group. Bars: 50 μm, Bax immunohistochemistry.

3. Results

The animal studied received a dose of Se (1.5 mg/kg) from the literature; the results of the acute toxicity test showed that no toxicity or death occurred in animals up to 23.0 mg/kg Se (LD_{50} value = 0). This supports the use of Se in healthy humans as a prophylactic antioxidant supplement [33]. In addition, LD_{50} values for B have been reported to be in the range of approximately 1700–3450 mg/kg body weight [34].

3.1. Body weights (BW) and liver weights (LW)

At the end of the experiment, a remarkable change was observed between the body weight groups (Fig. 1). The average BW was highest in the control group and lowest in the CP group. The body weights of the CP-treated group were lower compared to the control group (p < 0.05). Although the final body weights of the Se + CP and B + CP groups were higher, only the first group showed a significant difference compared to the CP group. A notable difference between the groups was found in LW (*p < 0.05*). The LW was highest in the Se and B groups and lowest in the CP group. The LW was lower in the CP group than in the control group and higher in the Se + CP and B + CP groups than in the CP group (Fig. 1). Regarding LW, no remarkable changes were observed between the groups (*p > 0.05*) (Fig. 1).

3.2. Histological results

Representative microscopic images obtained from the evaluation of liver sections stained with hematoxylin-eosin are shown in Fig. 2(a–f). According to the results, the liver tissue in the control, Se and B groups showed a typical histologic appearance (Fig. 2a and b and c). In the group receiving CP, degeneration of hepatocytes and congestion in the central veins were observed (Fig. 2 d). In the groups that received Se or B prior to CP administration, the histologic findings were similar to those in the control group. However, it was found that Se protected the liver slightly better from CP damage than B. This was due to the fact that some congestion was still present in the B group (Fig. 2e and f).
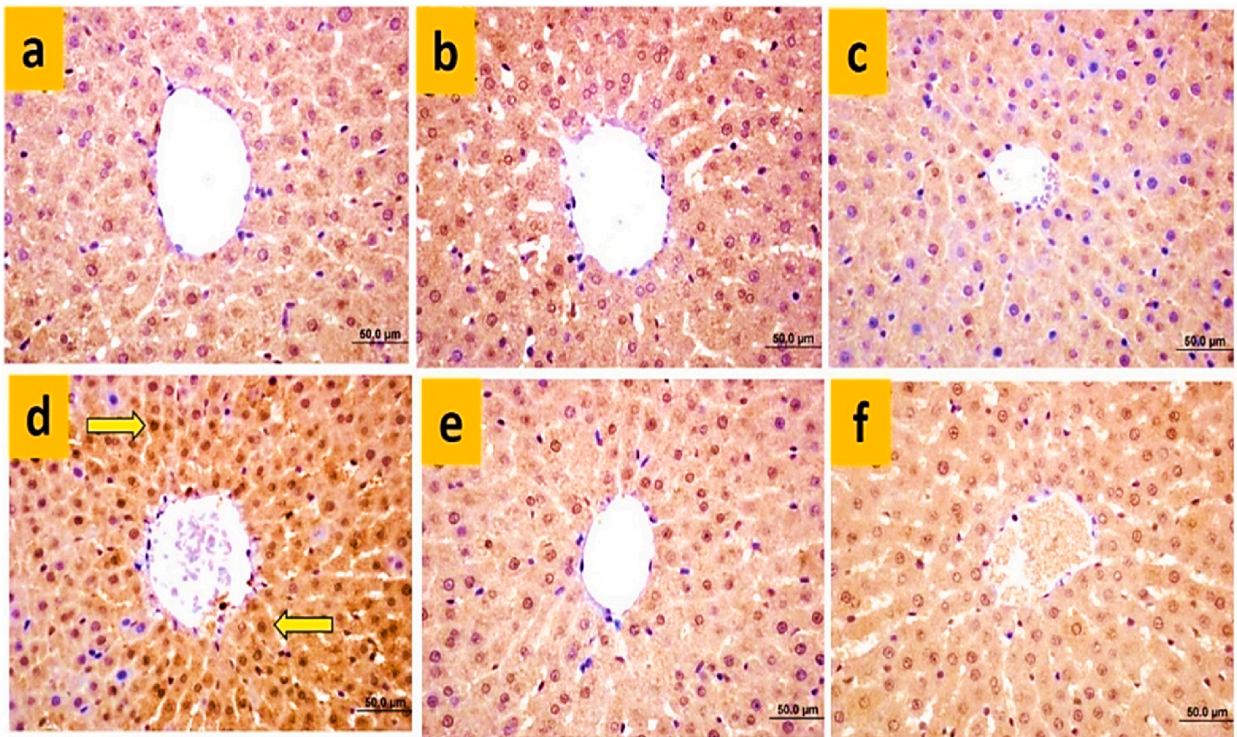
Fig. 4. Microscopic liver images according to experimental groups. Shown are the control group (a), the Se group (b), the B group (c), the CP group (d), the Se + CP group (e) and the B + CP group (f). It can be observed that there is no significant positive staining (apoptosis) in the control, Se, and B groups. In the CP group, there is positive staining of apoptotic hepatocytes (yellow arrows). Apoptosis was significantly reduced in the groups receiving Se or B prior to CP. Bars: 50 μm, caspase-3 immunohistochemistry.

3.3. Immunohistochemistry

3.3.1. Bax staining

Representative microscopic images obtained as a result of the evaluation of liver sections immunohistochemically stained with Bax are shown in Fig. 3(a–f). Accordingly, no significant apoptosis was detected in the liver tissues of the control, Se and B groups (Fig. 3a and b and c). In the group that received CP, positive staining (apoptosis) was observed in the hepatocytes (Fig. 3 d). When comparing the groups that received Se or B prior to CP administration, Se was found to significantly reduce apoptosis, while B was not as effective as Se in preventing apoptosis (Fig. 3e and f).

3.3.2. Caspase-3 staining

Fig. 4 (a-f) below shows some microscopic photographs taken during the assessment of liver sections immunohistochemically stained with caspase-3. No significant apoptosis was detected in the liver tissues of the control, Se and B groups (Fig. 4a and b and c). In the CP group, hepatocytes with positive staining (apoptosis) were detected (Fig. 4 d). Prior to CP administration, there was a significant decrease in apoptosis in the groups receiving Se or B (Fig. 4e and f).

3.3.3. Bcl-2 staining

An analysis of liver sections immunohistochemically labeled with the anti-apoptotic protein Bcl-2 yielded representative microscopic images (Fig. 5a–f). It was found that the liver tissue of the control, Se and B groups contained positively stained hepatocytes (Fig. 5a and b and c). The hepatocytes of the CP group showed no positive staining (Fig. 5 d). The groups that were administered Se or B prior to CP treatment also had positively stained hepatocytes (Fig. 5e and f).

3.3.4. Nrf2-Keap-1 staining

The next figure, Fig. 6(a–f), shows representative microscopic images taken after evaluation of liver slices stained with Nrf2 immunohistochemistry. The result is that the cytoplasm of the hepatocytes was positively stained in each group, but the nuclei were not stained in any of the groups. However, it is noteworthy that the staining in the other groups was not as strong as in the control group (Fig. 6a–f).

Fig. 7(a–f) shows representative microscopic images obtained from the evaluation of liver sections immunohistochemically stained with Keap-1. The result is that the cytoplasm of the hepatocytes of all groups were positively stained, but the nuclei of the hepatocytes
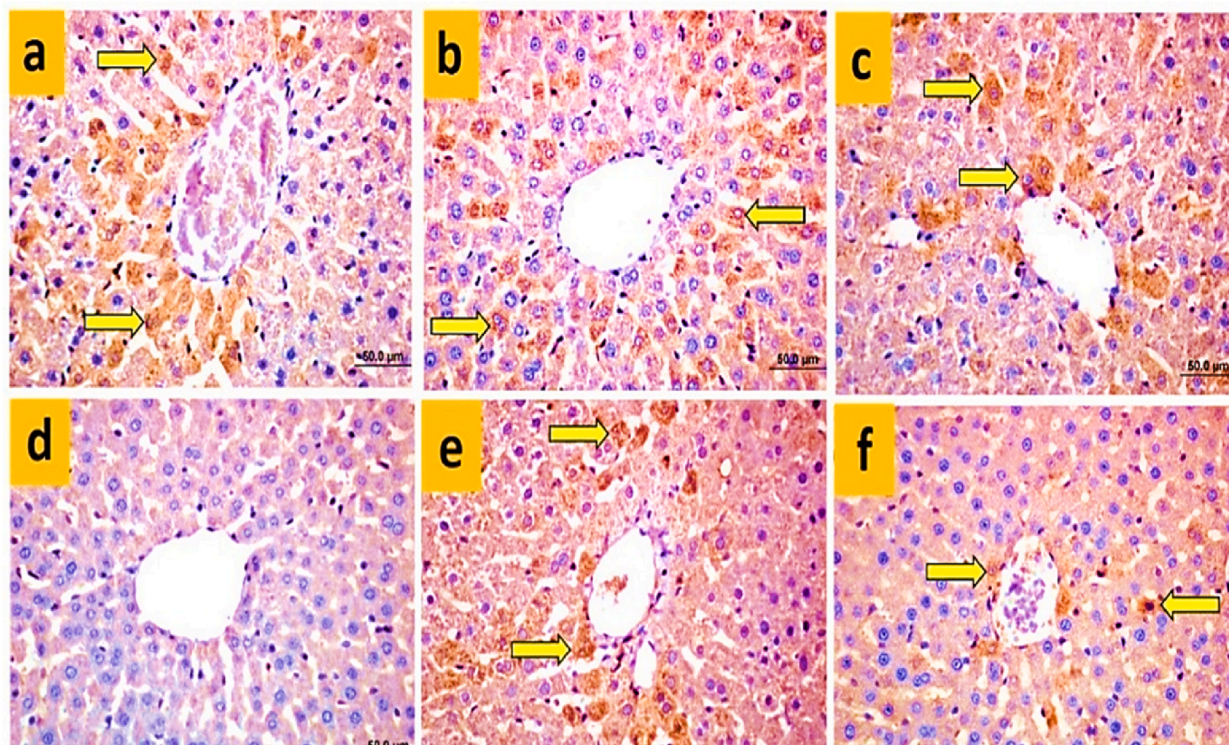
Fig. 5. Microscopic liver images according to experimental groups. Shown are the control group (a), the Se group (b), the B group (c), the CP group (d), the Se + CP group (e) and the B + CP group (f). Positive staining (yellow arrows) is observed in hepatocytes of the control, Se, and B groups. No positive staining was observed in the hepatocytes of the CP group. It can be seen that there are hepatocytes (yellow arrows) that are positively stained in the groups that received Se or B before CP. Bars: 50 μm, Bcl-2 immunohistochemistry.

in none of the groups showed positive staining. However, it is significant that the staining was less intense in the other groups than in the control group (Fig. 7a–f).

3.4. ALT, AST, ALP, TAS, TOS, and OSI results

Fig. 8 shows the serum levels of ALT, AST, ALP, TAS, TOS and OSI. When comparing the Se, B and control groups with the group receiving only CP, a statistically significant shift in serum levels of ALT, AST, ALP, TAS, TOS and OSI was observed. When the groups treated with Se + CP and B + CP were compared with the group treated with CP, a statistically significant difference was observed in the serum levels of ALT, AST, ALP, TAS, TOS and OSI. Nevertheless, Se was found to be more protective of the liver than B.

3.5. Levels of proinflammatory cytokines

Fig. 9 shows the serum levels of TNF-α, IL-1β, IL-6 and IL-10. Consequently, a statistically significant shift in serum levels of NF-kB, TNF-α, IL -1β, IL -6 and IL -10 was observed when the group receiving CP alone was compared with the Se, B and control groups. A statistically significant difference was observed in serum levels of NF-kB, TNF-α, IL -1β, IL -6 and IL -10 when the Se + CP and B + CP-treated groups were compared with the CP-treated group. However, the results showed that Se protects the liver more effectively than B due to its anti-inflammatory effect.

3.6. Results of SOD, CAT, GPx, MDA, and GSH levels in serum samples

The MPO, SOD, CAT, GPx, MDA and GSH levels in serum are shown in Fig. 10. A statistically remarkable change in serum levels of SOD, CAT, GPx, MDA and GSH was observed in the group receiving only CP compared to groups Se, B and the control.

When comparing the MPO, SOD, CAT, GPx, MDA and GSH values between the groups receiving Se + CP and B + CP and the group receiving CP, there was a statistically significant difference. Se was found to have a greater effect on preventing lipid peroxidation and improving the antioxidant defense system compared to B.
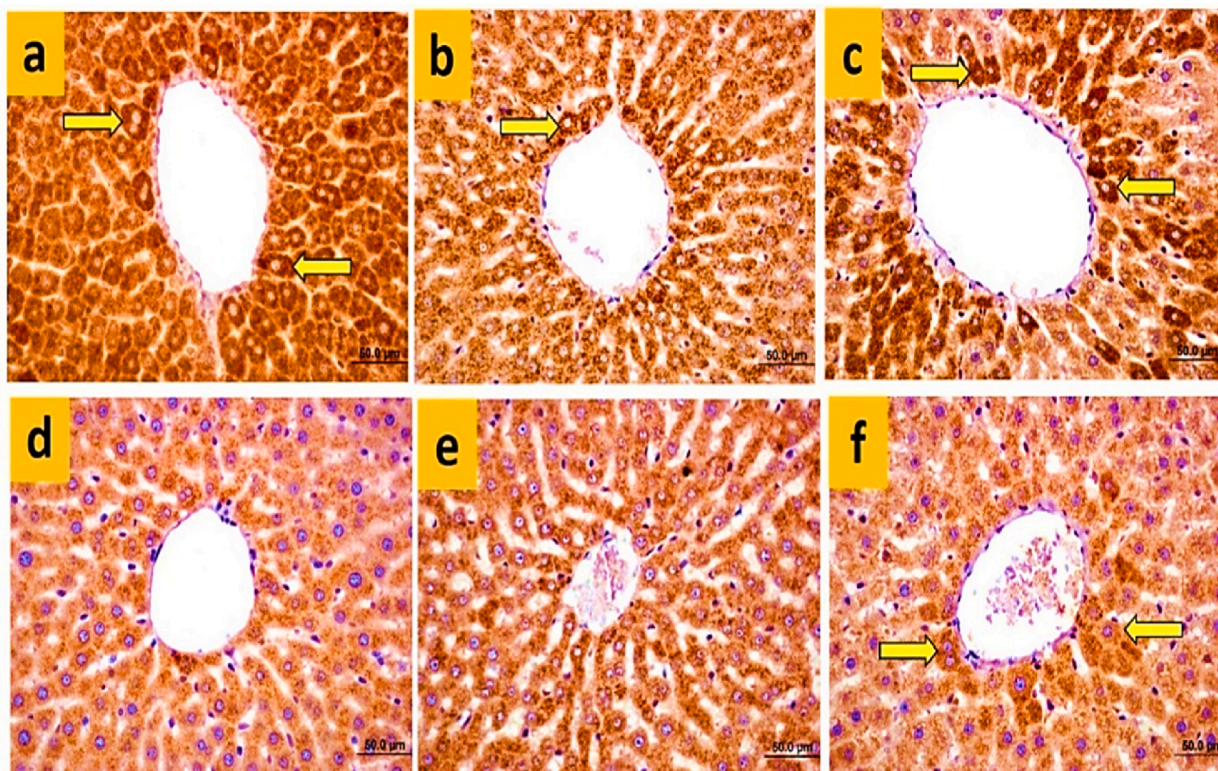
Fig. 6. Microscopic liver images according to experimental groups. Shown are the control group (a), the Se group (b), the B group (c), the CP group (d), the Se + CP group (e) and the B + CP group (f). It can be seen that the cytoplasm of hepatocytes is positively stained in all groups (yellow arrows), more clearly in the control group, but the nuclei of hepatocytes do not show positive staining in any group. Bars: 50 μm, Nrf2 immunohistochemistry.

3.7. Molecular docking results

3.7.1. Molecular docking and validation results for CuZnSOD

The molecular mechanism of the protective effect of Se and B against CP-induced damage was investigated by *in silico* studies, considering the crystal structure of CuZnSOD. Gibbs free energy changes, H-bonds interactions, Pi-Alkyl interactions, Cu-His61-Zn bridge ruptures/reformations, and bond lengths were determined for docking of CP, Se, and B into SOD. The summative results as presented in Table 2. The molecular docking results obtained based on the interactions of CP, Se and B with CuZnSOD are shown in 2D and 3D in Fig. 11.

The results of the validation study comparing the types of interactions and Gibbs free energy change values between CP, Se and B and CuZnSOD are shown in Fig. 12a and b. To investigate the type of interactions involved in the binding reaction, the stability of the activators (lactose, maltose, sucrose and trehalose) with the CuZnSOD protein complexes was evaluated considering the RMSD and hydrogen bonds (Fig. 12a and b). Fig. 12 a displays the findings of an analysis of the kinetics of the binding process and the flexibility of CuZnSOD.

On the other hand, the effects of CP on the activity of CAT and the changes in these effects due to Se and B doping were investigated separately by *in silico* studies (Fig. 13a–c). The results of *in silico* studies conducted to explain the detrimental effects of CP on the activity of CAT and the mechanism of action of Se and B to reduce these effects are summarized in Table 3. The interaction results for CP, Se and B with CAT amino acid residues were also shown in Fig. 13b and c. To evaluate the effects on the interaction mechanisms of CAT, molecular docking analyses of both interactions between B-CAT and Se-CAT were first performed; the results are shown in Fig. S3. 3D images of the docking results are shown in Fig. S4.

Glutathione (GSH) is a tripeptide antioxidant that protects cells from the toxic effects of reactive oxygen species and plays an important role in the detoxification of hydrogen peroxide and lipid peroxide by the enzyme GPx1. GPx (human erythrocyte GPx1, PDB code: 2F8A), a selenoprotein, is an antioxidant enzyme that tends to reduce hydroperoxides derived from lipids or non-lipids. The results of the *in silico* study explaining the inhibitory effect of CP on GPx1 activity and the mechanism of action of Se and B used to reduce this effect are shown in Fig. 14a–c. In addition, the evaluations of hydrogen bonding and hydrophobic interactions of both co-docking and separate docking of CP, Se and B into GPx1 are summarized in Table 4. To assess the impact on GPx1 interaction mechanisms, primarily the molecular docking results of the interactions between B and Se and GPx1 are shown in Fig. S5. On the other
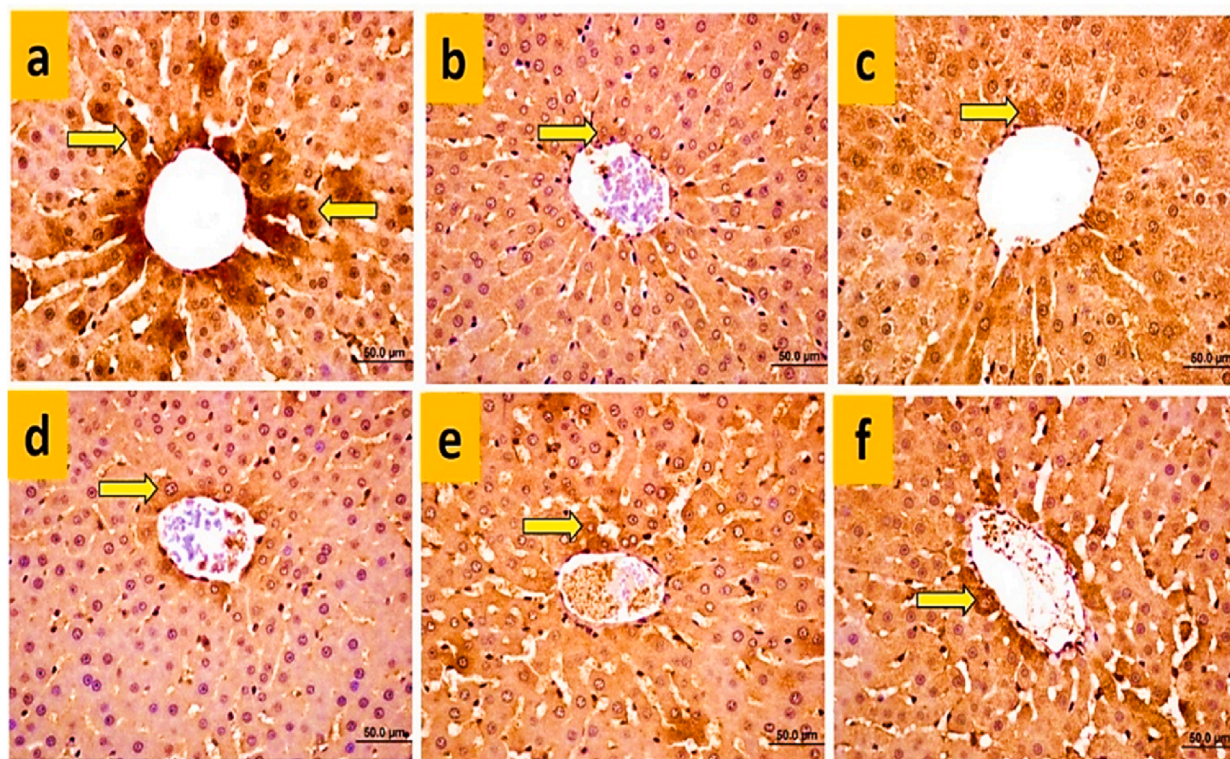
Fig. 7. Microscopic liver images according to experimental groups. Shown are the control group (a), the Se group (b), the B group (c), the CP group (d), the Se + CP group (e) and the B + CP group (f). It can be seen that the cytoplasm of hepatocytes is positively stained in all groups (yellow arrows), most clearly in the control group, but the nuclei of hepatocytes do not show positive staining in any group. Bars: 50 μm, Keap-1 immunohistochemistry.

hand, the effects of CP on GPx1 activity and the changes in these effects due to Se and B doping were investigated separately by *in silico* studies, and the docking results for possible binding sites are shown in Fig. 14a–c. The 3D images of the docking results are shown in Fig. S6.

4. Discussion

The results show that the CP group has the lowest mean values for LW. However, apart from the CP group, the mean values of the liver index showed no statistically significant difference between the groups. According to this result, CP is a risk for the whole body and also for the liver. When we look at the literature, we find that some studies on the effects of CP on liver weight have produced conflicting results. Goyal et al. reported that rats treated with CP had a significantly lower liver weight than the control group [35]. Adikwu and Bokolo found that CP did not significantly alter the wet weight of rat livers [36]. Similar to Goyal et al. [35], they found that rats treated with CP had significantly lower liver weights compared to rats in the control group. In the present study, the mean LW values were higher in the Se + CP and B + CP groups than in the CP-only group, suggesting that Se and B may have a protective effect against CP toxicity. This result is probably due to the neutralizing effect of Se and B on the toxicity of CP. There is no comparative study in the literature showing the effect of Se and B on the decrease in liver weight caused by CP. However, the toxic effect of CP on liver function could explain an increase in AST, ALT and ALP levels in the group receiving CP compared to the control group. ALP, ALT and AST levels have been shown to increase in response to CP [37,38]. The remarkable changes in these indicators suggest that CP causes liver cell damage and liver dysfunction [39]. In the present study, the levels of AST, ALT and ALP were significantly lower in the Se + CP and B + CP groups than in the CP group, which may indicate that Se and B improve liver functions. It is known that Se and B have the ability to restore the levels of AST, ALT and ALP. In other words, it can be stated that Se and B may have achieved this effect by protecting the integrity of the cell. Cengiz et al. [26] found the liver damage caused by CP in rats and the associated high levels of AST, ALT and ALP were compared with those after administration of B [26]. Methimazole was found to increase plasma transaminase activities and total, direct and indirect bilirubin levels. Co-administration of Se with diet improved all biochemical parameters [40]. In the CCl4-treated group, there was a significant increase in serum AST, ALP and ALT activities, indicating CCl$_4$-induced liver cell injury compared to the control group (p < 0.05). However, it was found that treatment with B at a dose of 200 mg/kg before CCl$_4$ reversed the CCl$_4$-induced change in AST, ALP and ALT (p < 0.05). Se and B could have this effect via lowering ROS levels, which may limit inflammatory processes and prevent apoptotic cell death, and increasing antioxidant levels, which may prevent GSH degradation. In
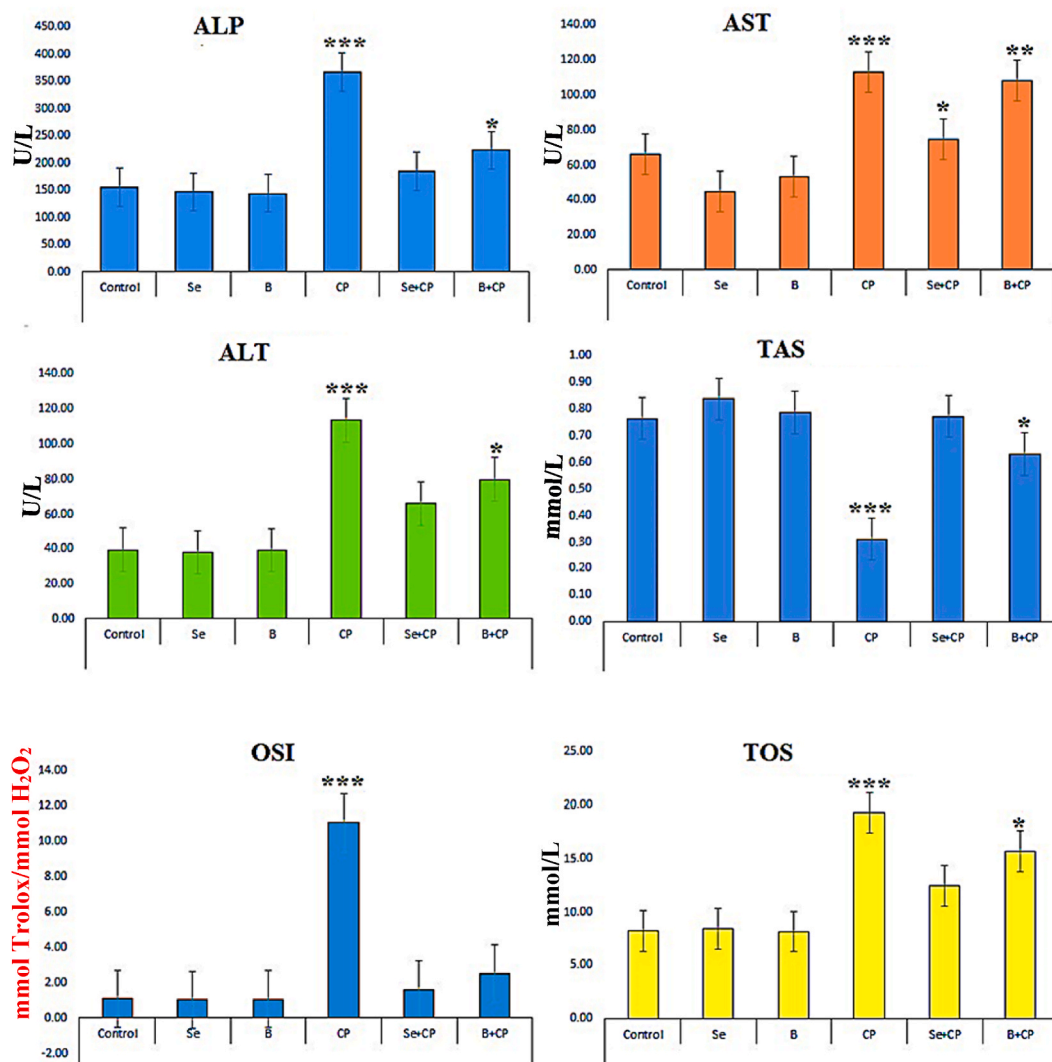
Fig. 8. Comparison of the values of ALT, AST, ALP, TAS, TOS, and OSI in all groups. ***; $p < 0.001$; There is a very notable change compared to the control group. **; $p < 0.01$; There is a remarkable change compared to the control group. *$p < 0.05$; There is a significant difference compared to the control group.

addition, it may have an indirect inhibitory effect on apoptosis [41].

Abnormalities in redox homeostasis have also been associated with various drug- and chemical-induced liver injury, including CP [42–59]. After CP therapy, free radical production attacks hepatocyte membranes and causes lipid peroxidation, which is a sign of oxidative insults and induction of cell damage [60]. In this current study, it had been found that the group receiving CP had the lowest levels of GSH, CAT, GPx-1, TOS and SOD and the highest levels of MDA and TAS, which increased the number of oxidative radicals, depletion of cellular antioxidant reserves, lipid peroxidation and consequent oxidative stress. The fact that the levels of GSH, GPx-1, TOS, CAT and SOD were higher in the Se + CP and B + CP groups than in the CP-only group, and that the levels of MDA and TAS were lower than in the CP-only group, suggests that B and Se increase intracellular antioxidant status. However, even with a small difference, Se was found to be more protective against CP-induced changes than B. In one study, CP administration resulted in a significant decrease in SOD, CAT and GSH and an increase in TBARS and nitrite levels, leading to oxidative stress [61]. Administration of CP resulted in a significant decrease in GSH levels, SOD, CAT and GST and an increase in MDA levels [62]. In a similar study, a significant ($p < 0.05$) decrease in liver enzymes SOD, CAT, GSH and GPx-1 were observed in rats administered CP compared to control [36]. Intraperitoneal administration of CP increased malonaldehyde levels, decreased glutathione levels and the activity of antioxidant enzymes (GPx1, glutathione transferase, SOD and CAT). Oral administration of Se significantly decreased MDA, ROS and glutathione levels and restored the activity of antioxidant enzymes [63]. In rats treated with CP alone, the levels of TOS and OSI increased, while TAC levels decreased. CP decreased when Se and biochemical results were processed together [64]. CP caused an increase in malondialdehyde and a decrease in the activities of CAT, GSH, SOD and antioxidant activities in plasma. In addition, B reversed all
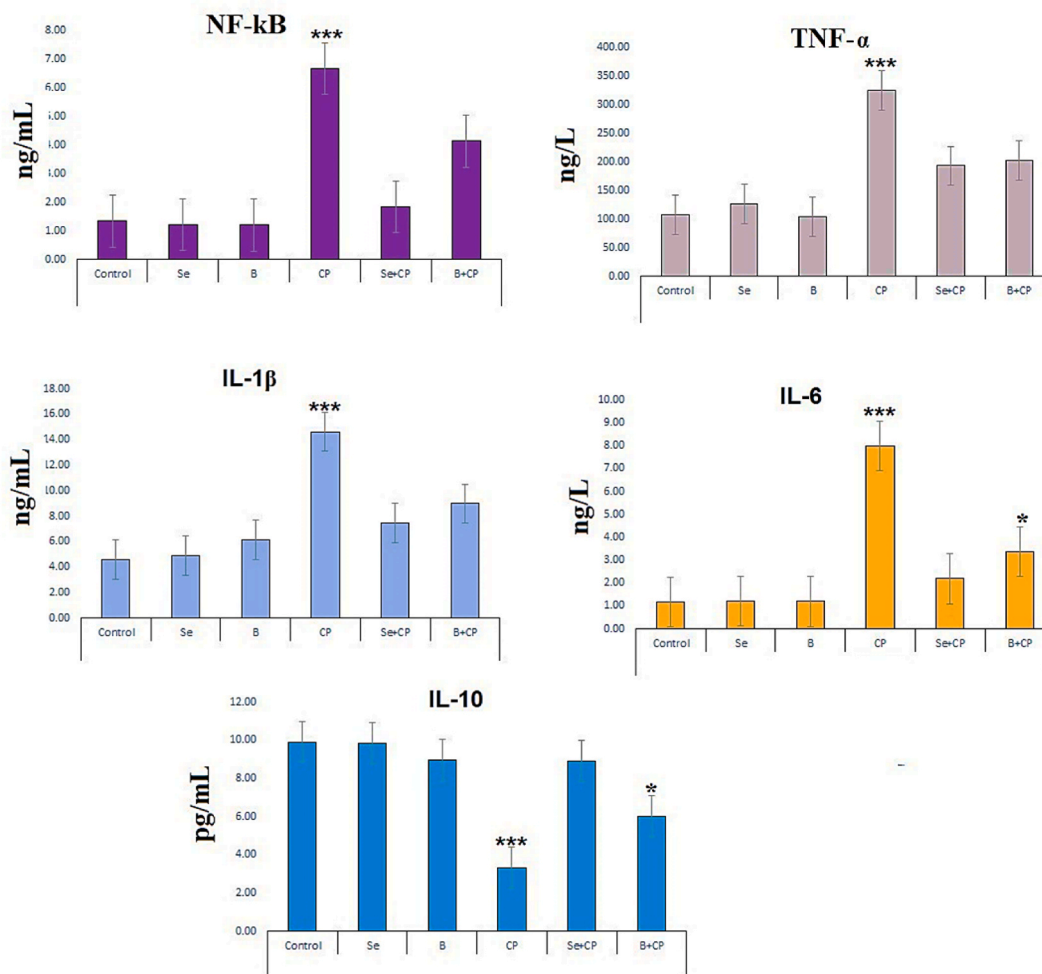
Fig. 9. Shows the effect of CP, Se, and B on the levels of NF-kB, TNF-α, IL -1β, IL -6, and IL -10. ***; p < 0.001; There is a very notable change compared to the control group. *p < 0.05; There is a significant difference compared to the control group.

changes induced by CP [65]. In agreement with the literature, our study group also indicates that B and Se support antioxidant capacity and prevent lipid peroxidation [13,21,64]. Consistent with the results of this study, previous studies in the literature have documented that Se and B can reduce free radical formation in experimental rats undergoing CP-induced liver injury [26,66].

In the present study, microscopic analysis of the livers of the CP group showed damage such as degeneration of degenerated hepatocytes and congestion that were larger and more conspicuous than in the other groups. Iqubal et al. demonstrated the biochemical and morphological effects of CP on the livers of albino rats and numerous changes such as necrosis, cell infiltration and hemorrhagic areas [61]. Mahmoud et al. reported the effects of CP on the liver of albino rats, extensive mononuclear infiltration, loss of cell margins, necrosis and massive loss of cytoplasm in the hepatocytes [67]. Here, we demonstrated the morphologic changes of the liver with degeneration similar to the two studies mentioned above. In fact, the histologic degeneration detected in the CP group was less in the B + CP and Se + CP groups, suggesting that B and Se also improve liver histology. These results are consistent with the studies of Kar et al. and the studies of Ince et al. [65,68]. The exact method by which Se and B may exert these protective effects is controversial. It is likely that Se and B prevent tissue damage by blocking lipid peroxidation and stimulating antioxidant enzymes [69,70]. The results of this study show that in liver sections stained with Nrf2-Keap-1 immunohistochemistry, the cytoplasm of hepatocytes was positively stained in all groups, whereas there was no positive staining in the nuclei of hepatocytes in any group. The results of this study appear to differ from those reported in the literature [71,72]. However, more detailed studies are needed to determine the reasons for this difference. Instead of acting as Nrf2 activators, B and Se might act as free radical scavengers for CP and reduce CP-induced toxicity and oxidative stress.

Several antineoplastic agents have been reported to activate the transcription factor NF-κB in addition to inflammation [73]. NF-κB is one of the most important transcription factors involved in the regulation of genes involved in the process of inflammation, cell proliferation and survival [73]. Akcay et al. [74] have shown that CP is related to the increased production of inflammatory mediators produced by the damaged or immune cell-induced leukocyte infiltration at the site of injury. Gao et al. demonstrated that ROS
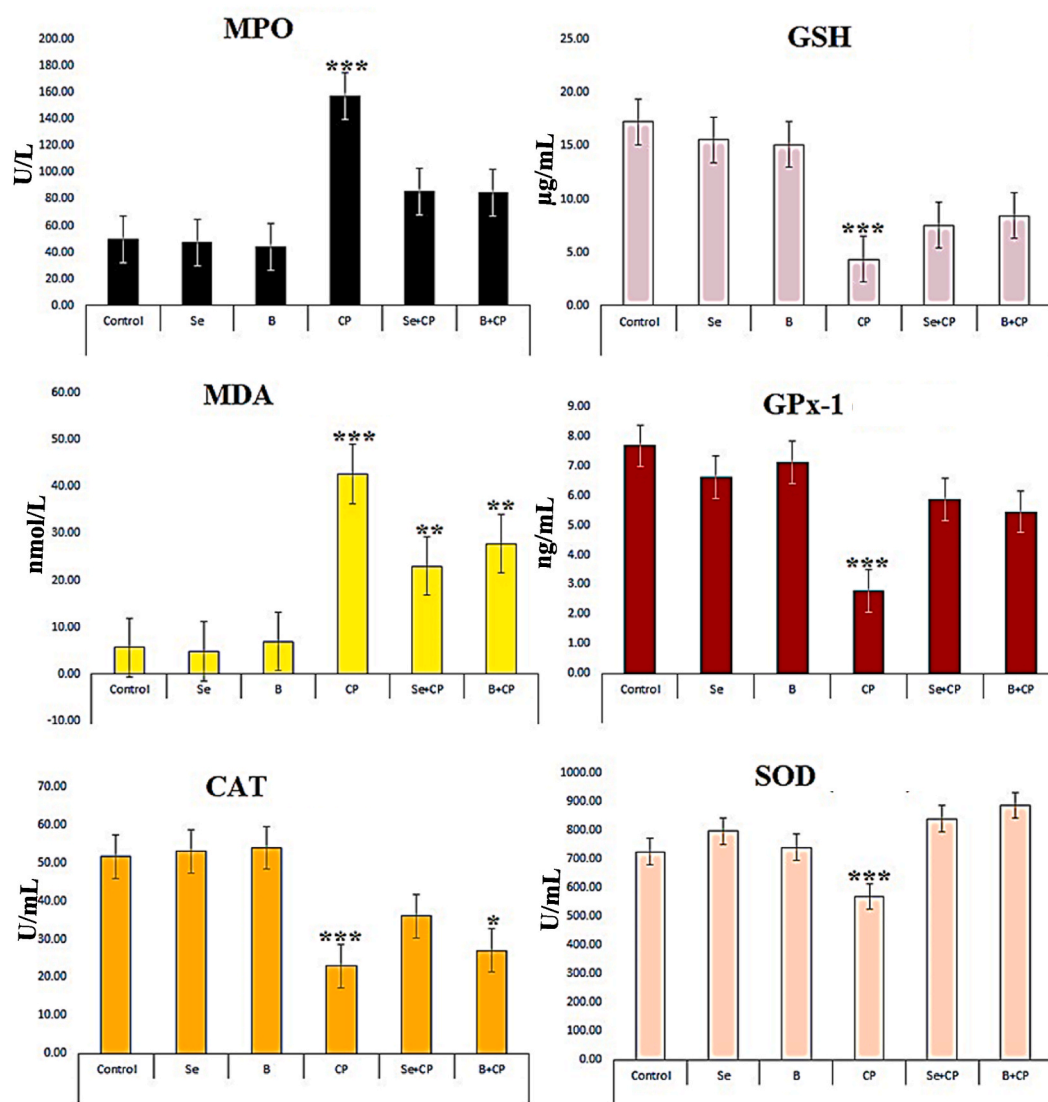
Fig. 10. The effect of CP, Se, and B on the level of MPO, SOD, CAT, GPx, MDA, and GSH. ***; $p < 0.001$; There is a very notable change compared to the control group. **; $p < 0.01$; There is a remarkable change compared to the control group.

increased the gene expression of inflammatory mediators and NF-κB [75], and Sami et al. reported that ROS increased the production of TNF-α from Kupffer cells [76]. Presented study, CP-treated rats showed a remarkable increase of TNF-α and IL-1β in serum. This phenomenon may be related to CP-induced upregulation of NF-κB. Comparable results have been shown in previous studies [77–79]. When rats were treated with CP (200 mg/kg), a significant increase in NF-κB p65, IL-6 and TNF-α levels was observed along with a decrease in IL-10 levels [80]. After treatment with Se and B, a significant decrease in NF-κB, TNF-α, IL-6 and IL-1 β levels and an increase in IL-10 levels were observed. However, Se had a better effect than B on the activation of CP-induced proinflammatory cytokines.

Consistent with the results of this study, many studies associated CP administration with apoptosis in the liver. Cengiz et al. [23] reported that immunohistopathologic analysis revealed that the levels of caspase-3 and Bax were increased in the CP group compared to the control group, while Bcl-2 levels decreased [23,81]. Alqahtani et al. investigated CP-induced apoptosis of hepatocytes and determined both gene and protein expression levels of the proapoptotic factors caspase-3 and Bax by immunohistochemistry. They treated the livers of rats with CP for two weeks and found that CP induced a remarkable increase in caspase-3 expression and protein levels [82]. Caglayan et al. demonstrated that CP induces the apoptotic and autophagic pathway by increasing the expression of cysteine aspartate-specific protease-3 and the concentration of light chain 3B (LC3B) and also increases the expression of 8-hydroxy-y-2′-deoxyguanosine (8-OHdG), the marker of oxidative DNA damage [73]. Cengiz et al. reported that Bcl-2 levels decreased in the CP group, while Bax and caspase-3 levels increased [38].

Table 2
Summative results of both co-docking and separate docking of CP, Se, and B into SOD.

Ligand	ΔG (Kcal/mol)	H-bonds	Pi-Alkyl	Cu-His61-Zn bridge rupture/reformation
Se	**−4.42**	**His78(2.54)**[a]	-	–
		Lys134 (2.16)		
		Lys134 (2.01)		
B	**−4.33**	Gly70 (2.07)	–	–
		Gly70 (2.17)		
		Asp122(2.04)		
CP	**−4.18**	Asn84(2.12)	–	–
Se + CP	−4.16	**CP:** Thr86 (1.79)	–	–
		Thr86 (2.81)		
		Ile94 (2.16)		
		Se: Lys134 (2.16)		
		Lys134 (2.01)		
		His78(2.54)[a]		
B + CP	−3.98	**B:** Gly70 (2.07)	–	–
		Gly70 (2.17)		
		Asp122(2.04)		
		CP: Asn84(2.09)		

[a] Active site amino acid residues of SOD. Se: Selenium, B: Boron, CP: Cyclophosphamide. ΔG values marked in bold are the best binding energy values (Lowest energy value).

According to the crystal structure of CuZnSOD, the molecular system investigated comprises the protein ligands of the first shell of Cu and Zn metal centers and the ligand of the second shell Asp122 [83]. Based on the molecular docking results for B and Se, the available sequences of the CuZnSOD macromolecule show strictly conserved residues in the active site region (Fig. S1 a, and b). Copper is coordinated by His44, His46, and His118 structural ligands, while zinc is coordinated by His69, His78, and Asp81 structural ligands. Both the Cu and Zn ions were included with His44, His46, His61, His69, His78, His118, and Asp81 ligands [83].

In the Se/CuZnSOD complex, His78, one of the amino acids His69, His78, and Asp81 responsible for the coordination of the Zn metal, entered into a conventional hydrogen-bonding interaction with Se in addition to this coordination. This situation was not observed in the interaction between B and SOD. The metal ions are separated by about 6.59 Å, and His61 plays an exceptional bridging role by coordinating Cu through HIS61 and zinc through His61. The lack of disruption of the His61 bridge for both Se and B suggests that the activity of SOD is not reduced in either case [84]. The ASP122 carboxylate provides additional stabilization of the dinuclear metal cluster by forming an indirect bridge via hydrogen bonds to both His44 and His69 [83].

Concerning B and Se doping, it was found that, unlike Se, a conventional hydrogen bonding interaction occurs between B and Asp122, whereas there is no such interaction with HIS44 and HIS69 (Fig. 11). This suggests that the contribution to the thermal stabilization of Asp122-induced SOD is eliminated in the B administration. Considering the changes in Gibbs free energy, we see that the calculated value for the formation of the Se/CuZnSOD complex (−4.42 kcal/mol) is lower (−4.33 kcal/mol) than for the formation of the B/CuZnSOD complex. Moreover, the lack of interaction between Se and the second-shell ligand (Asp122) suggests that Se increases the activity of SOD more than B. These results are also consistent with the *in vivo* results.

The molecular docking results of the CP/CuZnSOD complex showed that the coordination of the two metals was not changed by CP and that the Cu-His61-Zn bridge was not disrupted/reformed. As seen Fig. 11 a CP does not interact with Asp122, which also contributes to the stability of SOD. However, the CP was found to have binding outside the range of Cu ions, which are directly responsible for the catalytic activity of SOD, and Zn ions, which are indirectly responsible for the catalytic activity (Fig. S2 c). In addition, it can also be seen that CP interacts with SOD, especially with conventional hydrogen bonds, carbon-hydrogen (2) and alkyl (3). These results suggest that CP may have a negative effect on the activity of SOD, but not on its stability. Consistent with these results, the activity of SOD decreased significantly *in vivo*.

In silico studies of Se and CP molecules on CuZnSOD were performed, and it was evaluated whether the negative effect of CP on the activity of SOD could be prevented by Se; the results are shown in 2D in Fig. 11b and c. These interactions are shown in Fig. S2 in 3D.

In the *in silico* study of Se and CP molecules on CuZnSOD, Se did not affect the coordination of SOD with Cu and Zn, CP did not affect the Cu-HIS61-Zn imidazolate bridge in the active region of CuZnSOD, 3 conventional hydrogen bonding occurred, and it did not interact with Asp122 (Fig. 11 b). On the other hand, Fig. S2 shows that Se is located in the cave of the active center of SOD, while CP is located in a cave near the cave of the active center of SOD. Considering that the diameter of the active site cavity of CuZnSOD is about 4.0 Å, it can be seen that CP narrows the free volume in which the center of mass of the molecule required for the catalytic reaction of SOD can move. According to the Sackur−Tetrode equation, this leads to an increase in the translational entropy value, so an increase of ΔG is to be expected [83,85,86]. Considering Table 2, the ΔG value for CP was calculated as −4.18 kcal/mol, while this value increased to −4.16 kcal/mol as a result of the co-application of Se with CP. In conclusion, the co-administration of Se and CP was found to be consistent with the *in vivo* results that Se protects against the adverse effects of CP and somewhat supports the activity of SOD.

It was investigated whether the negative effect of CP on the activity of SOD can be prevented by using B as an alternative to Se, and the results were shown in 2D in Fig. 11 c and 3D in Fig. S2. Considering Table 2 and Fig. 11 c, it was found that in the B@CP/CuZnSOD complex that occurred by administrating B and CP together, B had a conventional hydrogen bonding interaction with ASP122 and CP had only a conventional hydrogen bonding interaction (CP -ASN84). Similar to the Se@ CP/CuZnSOD complex, it was observed that B did not affect the coordination of SOD with Cu and Zn and CP did not affect the Cu-His61-Zn imidazolate bridge in the active site of
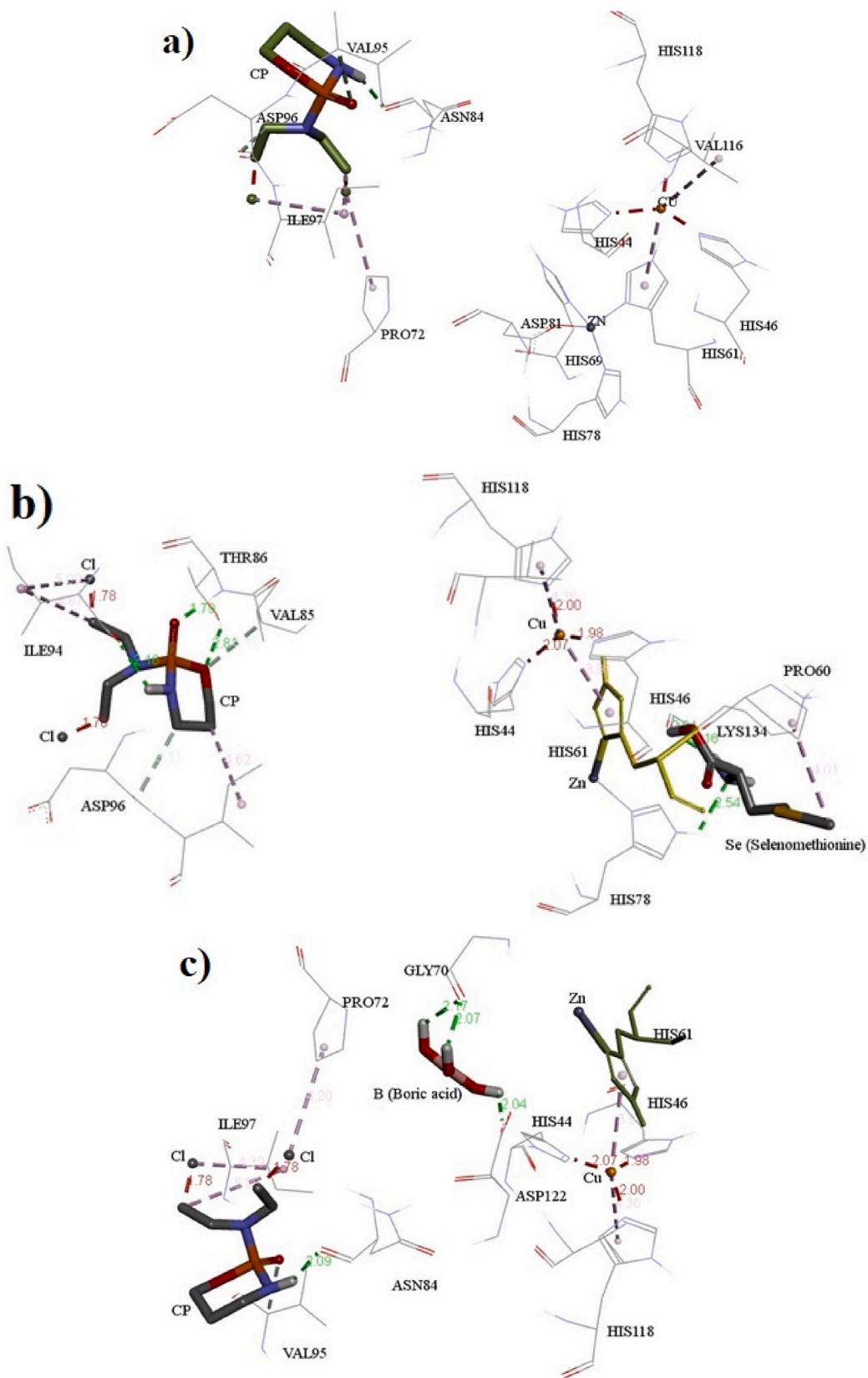
(caption on next page)

Fig. 11. Results of molecular docking due to the interaction of CP with CuZnSOD (2D representation): a) CP/CuZnSOD complex; b) Se@CP/CuZnSOD complex; c) B@CP/CuZnSOD complex.
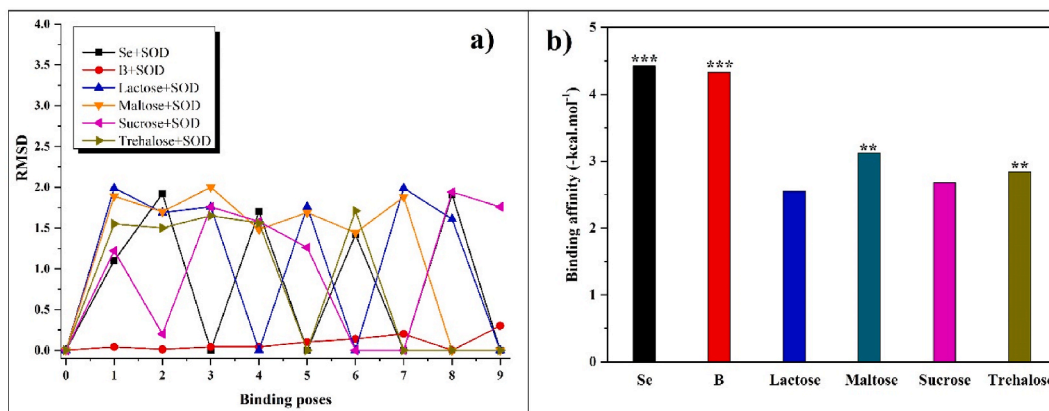

Fig. 12. Validation results based on the interaction of Se and B with the CuZnSOD macromolecule and specific CuZnSOD activators (lactose, maltose, sucrose, and trehalose): (a) Comparison of RMSD (Å) and binding affinity values; (b) Comparison of binding affinity values ((Quantitative value of ΔG from thermodynamic parameters calculated as a result of CuZnSOD interaction with the standard activators lactose, maltose, sucrose and trehalose (**); Se and B (***)).

CuZnSOD. However, the 3 conventional hydrogen bonds between CP-SOD in the Se@CP/CuZnSOD complex decreased to 1 for CP-SOD in the B@CP/CuZnSOD application. This indicates that the tolerance level of CP damage to SOD activity is better in B/CP application than in Se/CP application. This is also supported by the *in vivo* results.

On the other hand, comparing the Se/CP and B/CP applications, 6 conventional hydrogen bonds are formed in Se/CP, while 4 are formed in B/CP. This shows that the ΔG change of Se@ CP/CuZnSOD complexation is lower compared to B@CP/CuZnSOD, as this negatively affects the enthalpy and entropy changes. However, this value does not mean that it has a positive effect on the activity [83, 85,86].

Considering the validation studies (Fig. 11-a), it was determined that Se rather than B exhibited similar RMSD fluctuations as the standard CuZnSOD activators presented in the literature. On the other hand, Fig. 11-b shows that Se and B exhibited better negative binding energy values (−4.42 and −4.33 kcal/mol, respectively) compared to standard CuZnSOD activators (lactose, maltose, sucrose, and trehalose).

Compared to the ΔG values of CuZnSOD activators, Se and B showed lower values. Fig. 11-b shows that the best ΔG values belong to maltose and trehalose activators. All these results suggested that the binding affinity of CuZnSOD was greater to Se than to B, including maltose and trehalose activators. Validation studies show that the activator effect of Se on CuZnSOD activity may be stronger than specific CuZnSOD activators (lactose, maltose, sucrose, and trehalose).

Molecular docking studies have been repeated to demonstrate interactions between CP and CAT. CAT is an enzyme known to play a very important protective role against oxidative stress. Similar to our previous work, Se, B, and CP molecules were placed in one of the four identical subunits of CAT, each containing more than 500 amino acids with a porphyrin ring in the active site of heme [87]. The catalytic residues of CAT are Arg71, Val73, Phe333, Tyr357, and Arg364 [88]. Considering Fig. S3, it was found that Se interacted with the active site residues of CAT, but B did not. These results suggest that B contributes more to the activity of CAT compared with Se.

Looking at Fig. S4 a, it is clear that the CP is located in the cavity containing the amino acids responsible for the catalytic activity of the CAT. From Table 3 and Fig. 13 a, it is clear that CP primarily forms conventional H-bond interactions and pi-alkyl/alkyl interactions with all amino acid residues responsible for the catalytic activity of CAT. The value of the ΔG energy change due to these interactions was calculated to be −6.18 kcal/mol. Both the change in binding free energy and the binding with all amino acids of the catalytic cavity in the CP/CAT complex indicate that CP causes a decrease in the activity of CAT. From the 3D images (Figs. S4 b and c) obtained as a result of doping of CP with Se and BA, it is evident that CP forms hydrophobic interactions in regions outside the active site cavity of CAT. When Se and B are evaluated in terms of protection from damage to CP, CP can be expected to have fewer conventional hydrogen bonding interactions and weaker pi-alkyl interactions compared to B when Se is doped, which may indicate that Se provides more protection for the activity of CAT. This is consistent with the *in vivo* results.

GPx1, which is involved in all reactions of detoxification of hydrogen peroxide into water and lipid peroxides into alcohols, performs its function with the help of two glutathione molecules in a two-step process. The selenocysteine residue in the active site is important in this process. However, it has been reported that the active site selenocysteine is mutated to glycine (Gly47) in the crystal structure of GPx1 (2F8A) [89,90]. Therefore, Gly47 was considered to be an active site selenocysteine residue in *in silico* studies. In addition, Janetzki et al. reported residues Gly47, Arg52, and Arg179 as catalytic triads for GPx1 (2F8A) and amino acid residues Gln82 and Trp160 as inhibitor binding sites [90]. In addition, Trp160, Arg179, and Phe181 were identified as important amino acids for the glutathione redox reaction. The molecular docking studies aimed to investigate the effect of CP on GPx1 activity, which plays an
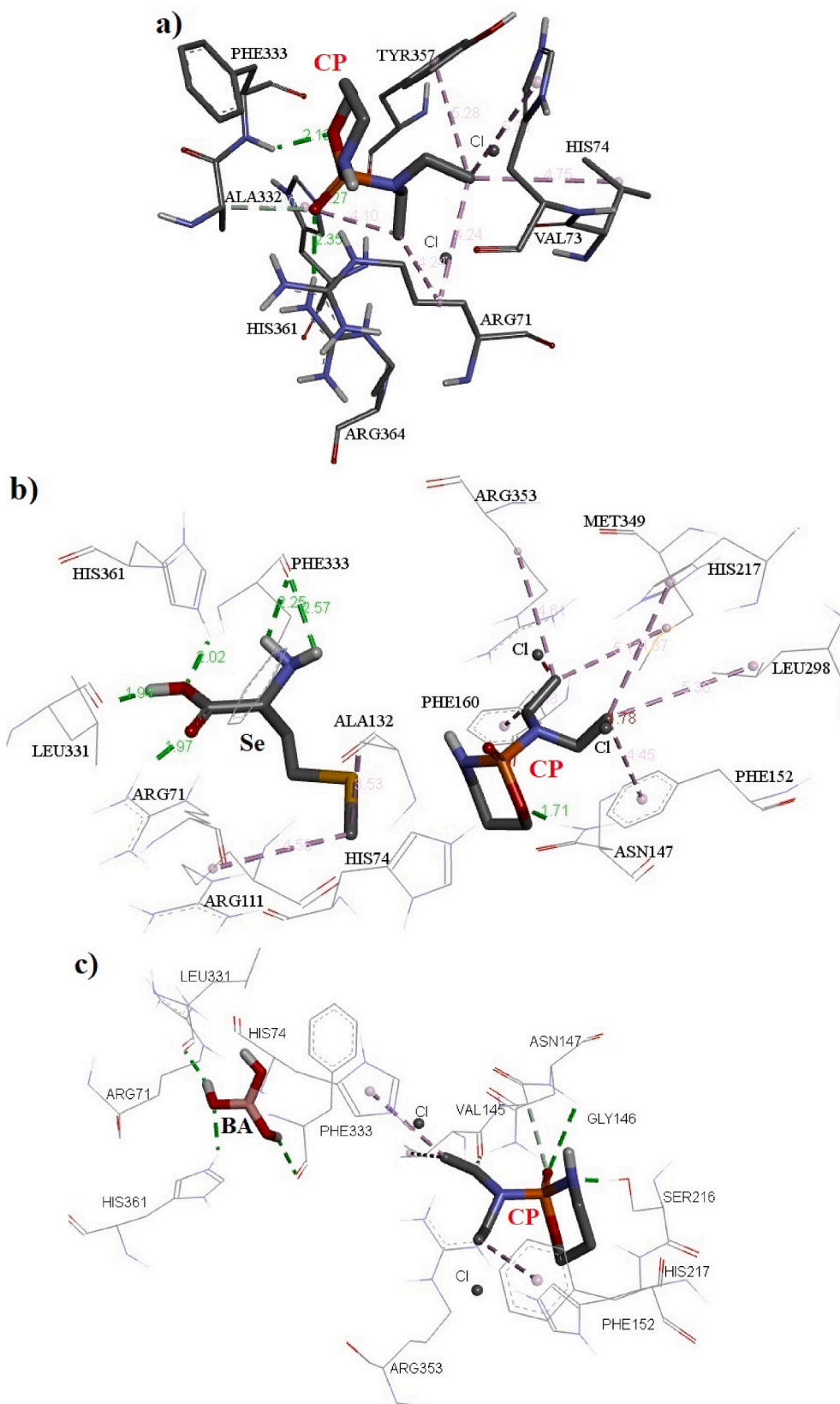
(caption on next page)

Fig. 13. Molecular docking results due to the interaction of CP, Cp&Se and CP &B with CAT (2D representation): a) CP @CAT complex; b) CP &Se@ CAT complex; c) CP &B@ CAT complex.

Table 3
Summative results of both co-docking and separate docking of CP, Se, and B into CAT.

Ligand	ΔG (kcal/mol)	H-bonds	Pi-Alkyl
Se	**−6.73**	**Arg71(1.97)**[a], **Phe333(2.25)**[a], **Phe333(2.57)**[a], Hıs361 (2.02), Leu331 (1.94)	–
B	**−4.78**	Thr218 (1.84), Lys232 (1.94), Asp297(1.86), Asp347(2.05), Asp347 (2.08)	–
CP	**−6.18**	**Phe333(2.12)**[a], Hıs361 (2.27), **Arg364(2.35)**[a]	**Hıs74(5.30)**[a], **Phe333(4.15)**[a], **Tyr357(5.28)**[a], Hıs361 (4.10),
Se + CP	−5.70	**Se: Arg71(1.97)**[a], Leu331 (1.94), **Phe333(2.25)**[a], **Phe333(2.57)**[a], Hıs361 (2.02) **CP:** Asn147(1.71)	**Se:** Phe160(4.48) **CP:** Phe152(4.45), Hıs217 (4.87)
B + CP	−5.05	**B:** Leu331 (2.05), **Phe333(2.26)**[a], Hıs361 (2.06) **CP:** Asn147(2.95), Ser216(1.67)	**B: None** **CP:** Hıs74 (4.33), Phe152(4.11)

[a] Active site amino acid residues of CAT. Se: Selenium, B: Boron, CP: Cyclophosphamide. ΔG values marked in bold are the best binding energy values (Lowest energy value).

important role in protecting the organism from oxidative damage, and to predict the protective aspects of Se and B on the activity. Docking studies of Se, B, and CP molecules were performed by targeting the active site residues of one of the two identical 184 amino acid subunits of GPx1. Fig. S5 a shows that Se does not interact with the selenocysteine residue (Gly47) of GPx1 and the active site residues of the catalytic triad. Fig. S5 b shows that B has two distinct effects on GPx. One is that B interacts with Gln82 and Trp160 to block inhibitory binding residues in GPx1 inhibition. The other effect is to interact with Gly48, the neighbor of Gly47 that functions as selenocysteine at the active site, and Trp160, the glutathione disulfide binding site. These interactions can be interpreted as a decrease in the GPx1 activity of B.

Considering Fig. S6 a, it is clear that the CP is located in the cavity containing the selenocysteine residue of GPx1, which contains the amino acids responsible for the catalytic activity. CP does not bind to the amino acids of the catalytic triad (Gly47, Arg52 and Arg179) and the glutathione disulfide binding sites of GPx1. However, conventional hydrogen bonding, alkyl, and other interactions with other amino acids in the cavity containing these amino acid residues indicate that the binding site of the glutathione tripeptide is blocked, resulting in a decrease in activity. Gibbs free energy exchange values obtained as a result of doping Se and B with CP showed that the protective effect of CP on the decrease of GPx1 activity could be stronger at B compared with Se. This is because when B and CP were applied together, there was an increase in the ΔG value (from −4.32 kcal/mol to −4.38 kcal/mol) and the affinity of GPx1 for CP decreased. While the *in silico* results for SOD and CAT were found to be fully compatible with the *in vitro* results, the *in silico-in vitro* compatibility for GPx1 was less pronounced.

5. Conclusion

This study demonstrated that CP can cause liver injury through oxidative stress, inflammation, and apoptosis. According to our *in vivo* and *in silico* results, Se and B treatment can protect rat liver tissue from CP-induced oxidative stress, inflammation, and apoptosis by regulating Bax/Bcl-2 and Nrf2-Keap-1 signaling pathways. In conclusion, Se showed a better effect than 20 mg/kg B in the prevention of liver toxicity caused by CP. Supplementation with Se and B could be a possible way to alleviate the liver damage caused by CP. More research using other molecular biomarkers should be conducted to increase therapeutic applicability and potential clinical benefit.

Funding

Data availability statement

No data was used for the research described in the article. This article has all the data that was created or evaluated during this investigation.

Ethics approval and consent to participate

The study was conducted based on the permit of Animal Experiments Local Ethics Committee of Eskişehir Osmangazi University (No: 148/776-1/2020 and 776-2/2022).
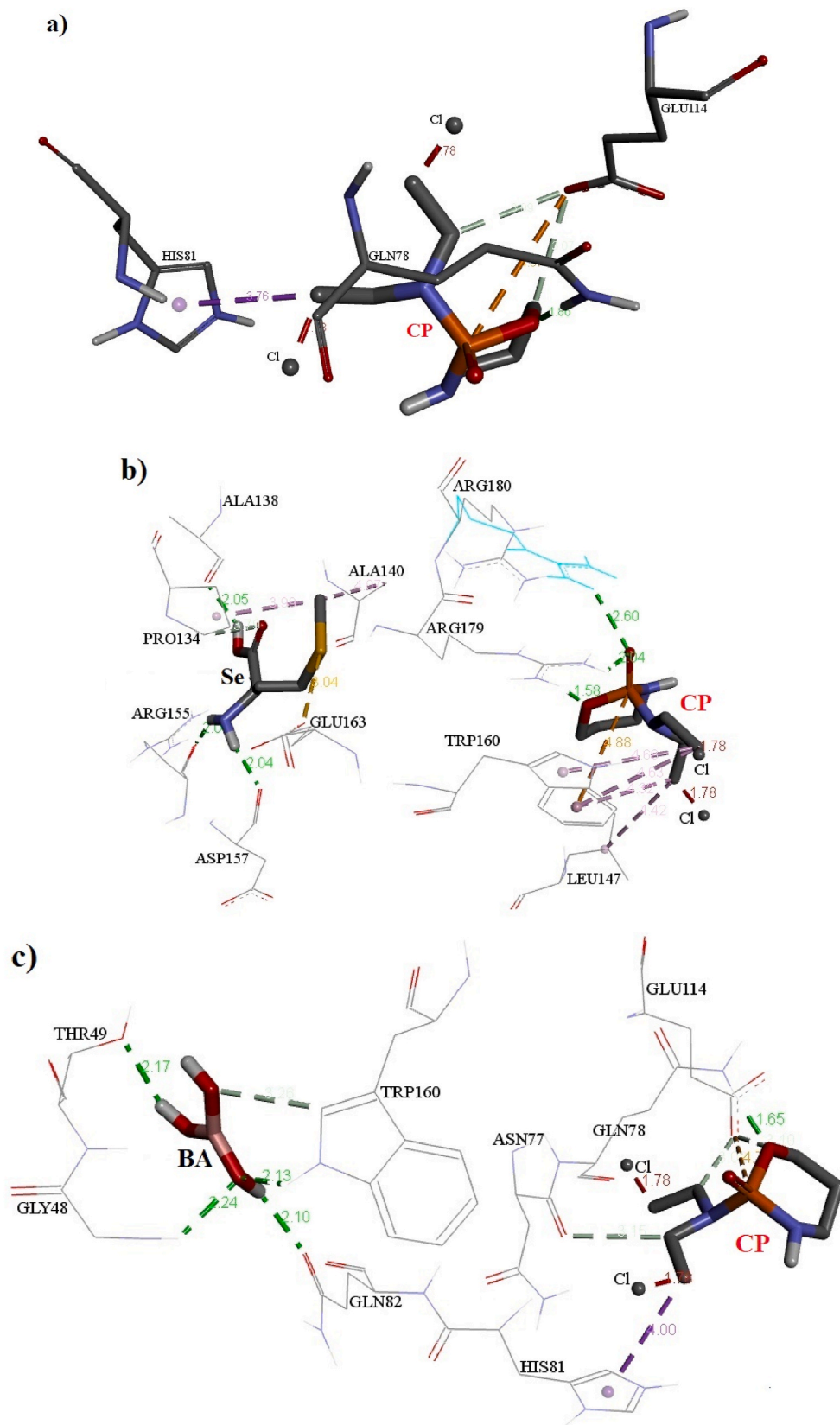
Fig. 14. Molecular docking results due to the interaction of CP, CP&Se, and CP &B with GPx1 (2D representation): a) CP @ GPx1 complex; b) CP &Se® GPx1 complex; c) CP &B@ GPx1 complex. Se: Selenium, B: Boron, CP: Cyclophosphamide.

Table 4

Summative results of both co-docking and separate docking of CP, Se, and B into GPx1.

Ligand	ΔG (kcal/mol)	H-Bonds	Pi-Alkyl
Se	−5.97	Arg155 (2.04), Asp157 (2.04), Ala138 (2.05)	–
B	−4.95	Gly48 (2.24), Thr49 (2.17), Gln82 (2.11), Trp160 (2.13)	–
CP	−4.32	Gln78 (1.86)	–
Se + CP	−3.24	Se: Ala138 (2.05), Arg155 (2.04), Asp157(2.04)	Se: None
		CP: Arg179 (1.58), Arg179 (2.04), Arg180 (2.60)	CP: Trp160 (4.68), Trp160 (4.32), Trp160 (4.63)
B + CP	−4.38	BA: Gly48 (2.24), Trp160 (2.13), Thr49 (2.17), Gln82 (2.11)	–
		CP: Gln78 (1.65)	

Se: Selenium, B: Boron, CP: Cyclophosphamide.

Consent for publication

Not applicable.

CRediT authorship contribution statement

Mustafa Cengiz: Writing – original draft, Resources, Project administration, Methodology, Investigation, Formal analysis, Data curation, Conceptualization. **Bahri Gür:** Resources, Formal analysis, Data curation, Conceptualization. **Fatma Gür:** Project administration, Methodology, Conceptualization. **Varol Şahintürk:** Resources, Methodology, Investigation. **Alpaslan Bayrakdar:** Methodology, Investigation. **Ilknur Kulcanay Şahin:** Resources, Project administration, Conceptualization. **Sıla Appak Başkoy:** Resources, Methodology. **Namık Bilici:** Methodology, Investigation. **Suzan Onur:** Resources, Methodology. **Yağmur Kaya:** Resources, Project administration, Methodology. **İsa Kıran:** Methodology, Investigation. **Özge Yıldırım:** Methodology, Conceptualization. **Nur Banu Akkaya:** Investigation. **Canan Vejselova Sezer:** Methodology, Investigation. **Adnan Ayhanci:** Resources, Project administration, Methodology, Investigation, Funding acquisition, Formal analysis, Data curation, Conceptualization.

Declaration of competing interest

The authors declare the following financial interests/personal relationships which may be considered as potential competing interests: Adnan Ayhanci reports financial support was provided by Eskisehir Osmangazi University. If there are other authors, they declare that they have no known competing financial interests or personal relationships that could have appeared to influence the work reported in this paper.

Acknowledgments

Appendix A. Supplementary data

Supplementary data to this article can be found online at https://doi.org/10.1016/j.heliyon.2024.e38713.

References

[1] A.A. El-Sheikh, M.A. Morsy, A.M. Okasha, Inhibition of NF-κB/TNF-α pathway may be involved in the protective effect of resveratrol against cyclophosphamide-induced multi-organ toxicity, Immunopharmacol. Immunotoxicol. 39 (2017) 180–187.

[2] P. Taslimi, F.M. Kandemir, Y. Demir, M. İleritürk, Y. Temel, C. Caglayan, İ. Gulçin, The Antidiabetic and Anticholinergic Effects of Chrysin on Cyclophosphamide-Induced Multiple Organ Toxicity in Rats: Pharmacological Evaluation of Some Metabolic Enzyme Activities, vol. 33, 2019 e22313.

[3] M. Cengiz, Ratlarda siklofosfamid nedenli kardiyotoksisite üzerine borik asitin koruyucu etkileri, Bitlis Eren Üniversitesi Fen Bilimleri Dergisi 7 (2018) 113–118.

[4] L.H. Fraiser, S. Kanekal, J.P. Kehrer, Cyclophosphamide toxicity, Drugs 42 (1991) 781–795.

[5] G.T. Budd, R. Ganapathi, L. Wood, J. Snyder, D. McLain, R.M. Bukowski, Approaches to managing carboplatin-induced thrombocytopenia: focus on the role of amifostine, Semin. Oncol. (1999) 41–50.

[6] A. Ayhanci, S. Günes, V. Sahinturk, S. Appak, R. Uyar, M. Cengiz, et al., Seleno L-methionine acts on cyclophosphamide-induced kidney toxicity, Biol. Trace Elem. Res. 136 (2010) 171–179.

[7] O. Özbakır, Occupational health and safety risk assessment and mitigation in chemistry laboratories: a case study of Iğdır University, Şırnak Üniversitesi Fen Bilimleri Dergisi 4 (2023) 1–20.

[8] X. Zhai, Z. Zhang, W. Liu, B. Liu, R. Zhang, W. Wang, et al., Protective effect of ALDH2 against cyclophosphamide-induced acute hepatotoxicity via attenuating oxidative stress and reactive aldehydes, Biochem. Biophys. Res. Commun. 499 (2018) 93–98.

[9] P. Mahipal, R.S. Pawar, Nephroprotective effect of Murraya koenigii on cyclophosphamide induced nephrotoxicity in rats, Asian Pac. J. Tropical Med. 10 (2017) 808–812.

[10] C. Singh, C. Prakash, K.N. Tiwari, S.K. Mishra, V. Kumar, Premna integrifolia ameliorates cyclophosphamide-induced hepatotoxicity by modulation of oxidative stress and apoptosis, Biomed. Pharmacother. 107 (2018) 634–643.

[11] S. Senthilkumar, T. Devaki, B.M. Manohar, M.S. Babu, Effect of squalene on cyclophosphamide-induced toxicity, Clin. Chim. Acta 364 (2006) 335–342.

[12] F. Gür, M. Cengiz, H.M. Kutlu, B.P. Cengiz, A. Ayhancı, Molecular docking analyses of Escin as regards cyclophosphamide-induced cardiotoxicity: in vivo and in Silico studies, Toxicol. Appl. Pharmacol. 411 (2021) 115386.

[13] M. Cengiz, Boric acid protects against cyclophosphamide-induced oxidative stress and renal damage in rats, Cell. Mol. Biol. 64 (2018) 11–14.

[14] M. Panahi-Kalamuei, M. Salavati-Niasari, S.M. Hosseinpour-Mashkani, Facile microwave synthesis, characterization, and solar cell application of selenium nanoparticles, J. Alloys Compd. 617 (2014) 627–632.

[15] F.A. Al-Salmi, R.Z. Hamza, Efficacy of vanadyl sulfate and selenium tetrachloride as anti-diabetic agents against hyperglycemia and oxidative stress induced by diabetes mellitus in male rats, Curr. Issues Mol. Biol. 44 (2021) 94–104.

[16] L. Xu, Y. Lu, N. Wang, Y. Feng, The role and mechanisms of selenium supplementation on fatty liver-associated disorder, Antioxidants 11 (2022) 922.

[17] L. Zhang, J.-Y. Xu, Y. Wei, S.-L. Gao, L. Wang, J.-Y. Zheng, et al., Protective effect of selenium-enriched green tea on carbon tetrachloride-induced liver fibrosis, Biol. Trace Elem. Res. 200 (2022) 2233–2238.

[18] A. Ayhanci, N. Heybeli, İ.K. Sahin, M. Cengiz, Myelosuppression and oxidative stress induced by cyclophosphamide in rats: the protective role of selenium, Adıyaman University Journal of Science 9 (2019) 252–265.

[19] G. Başaran, Obez Sıçanlarda Selenyum ve N-Asetil Sisteinin Fertilite/İnfertilite ve Karaciğer Üzerine Etkisi: Sağlık Bilimleri Enstitüsü, 2019.

[20] B.K. Shimada, N. Alfulaij, L.A. Seale, The impact of selenium deficiency on cardiovascular function, Int. J. Mol. Sci. 22 (2021) 10713.

[21] A. Ayhanci, D.T. Tanriverdi, V. Sahinturk, M. Cengiz, S. Appak-Baskoy, I.K. Sahin, Protective effects of boron on cyclophosphamide-induced bladder damage and oxidative stress in rats, Biol. Trace Elem. Res. 197 (2020) 184–191.

[22] M. Cengiz, O. Baytar, Ö. Şahin, H.M. Kutlu, A. Ayhanci, C. Veyiselova Sezer, B. Gür, Biogenic synthesized bare and boron-doped copper oxide nanoparticles from Thymbra spicat ssp. spicata: in silico and in vitro studies, J. Cluster Sci. (2023) 1–20.

[23] M. Cengiz, H.M. Kutlu, B. Peker Cengiz, A. Ayhancı, Escin attenuates oxidative damage, apoptosis and lipid peroxidation in a model of cyclophosphamide-induced liver damage, Drug Chem. Toxicol. 45 (2022) 1180–1187.

[24] H. Balaban, M. Nazıroğlu, K. Demirci, İ.S. Övey, The protective role of selenium on scopolamine-induced memory impairment, oxidative stress, and apoptosis in aged rats: the involvement of TRPM2 and TRPV1 channels, Mol. Neurobiol. 54 (2017) 2852–2868.

[25] F.K. Coban, S. Ince, I. Kucukkurt, H.H. Demirel, O. Hazman, Boron attenuates malathion-induced oxidative stress and acetylcholinesterase inhibition in rats, Drug Chem. Toxicol. 38 (2015) 391–399.

[26] M. Cengiz, A. Ayhanci, E. Akkemik, İ.K. Şahin, F. Gür, A. Bayrakdar, et al., The role of Bax/Bcl-2 and Nrf2-Keap-1 signaling pathways in mediating the protective effect of boric acid on acrylamide-induced acute liver injury in rats, Life Sci. 307 (2022) 120864.

[27] S. Zheng, A. Hameed Sultan, P.T. Kurtas, L.A. Kareem, A. Akbari, Comparison of the effect of vitamin C and selenium nanoparticles on gentamicin-induced renal impairment in male rats: a biochemical, molecular and histological study, Toxicol. Mech. Methods 33 (2023) 260–270.

[28] F. Gür, M. Cengiz, B. Gür, O. Cengiz, O. Sarıçiçek, A. Ayhanci, Therapeutic role of boron on acrylamide-induced nephrotoxicity, cardiotoxicity, neurotoxicity, and testicular toxicity in rats: effects on Nrf2/Keap-1 signaling pathway and oxidative stress, J. Trace Elem. Med. Biol. 80 (2023) 127274.

[29] D.B. Donmez, S. Kacar, R. Bagci, V. Sahinturk, Protective effect of carnosic acid on acrylamide-induced liver toxicity in rats: mechanistic approach over Nrf2-Keap1 pathway, J. Biochem. Mol. Toxicol. 34 (2020) e22524.

[30] A. Aycicek, O. Erel, Total oxidant/antioxidant status in jaundiced newborns before and after phototherapy, J. Pediatr. 83 (2007) 319–322.

[31] X. Ma, D. Deng, WJEi Chen, Inhibitors and Activators of SOD, GSH-Px, and CAT, vol. 29, 2017, p. 207, activators.

[32] L. Ferencz, D.L. Muntean, Potential inhibitors for bacterial dihydropteroate synthase. The results of a comprehensive screening based on structural similarity with p-amino-benzoic acid and docking simulation on the surface of enzyme, Rev. Roum. Chem. 59 (2014) 733–738.

[33] A. Shams, Y.M. Elbastawisy, N.E. Helal, Protective role of selenium against thyroid toxicity induced by lithium carbonate in albino rats: biochemical and immunohistochemical study, Egyptian Academic Journal of Biological Sciences, D Histology Histochemistry 15 (2023) 101–131.

[34] C.C. Pfeiffer, L.F. Hallman, I. Gersh, Boric acid ointment: a study of possible intoxication in the treatment of burns, J. Am. Med. Assoc. 128 (1945) 266–274.

[35] Y. Goyal, A. Koul, P. Ranawat, Ellagic acid ameliorates cisplatin induced hepatotoxicity in colon carcinogenesis, Environ. Toxicol. 34 (2019) 804–813.

[36] E. Adikwu, B. Bokolo, Effect of cimetidine on cyclophosphamide-induced liver toxicity in albino rats, Asian J. Med. Sci. 9 (2018) 50–56.

[37] C. Caglayan, The effects of naringin on different cyclophosphamide-induced organ toxicities in rats: investigation of changes in some metabolic enzyme activities, Environ. Sci. Pollut. Control Ser. 26 (2019) 26664–26673.

[38] M. Cengiz, S.C. Yildiz, C. Demir, İ.K. Şahin, Ö. Teksoy, A. Ayhanci, Hepato-preventive and anti-apoptotic role of boric acid against liver injury induced by cyclophosphamide, J. Trace Elem. Med. Biol. 53 (2019) 1–7.

[39] Y. Temel, S. Kucukler, S. Yıldırım, C. Caglayan, F.M. Kandemir, Protective effect of chrysin on cyclophosphamide-induced hepatotoxicity and nephrotoxicity via the inhibition of oxidative stress, inflammation, and apoptosis, N. Schmied. Arch. Pharmacol. 393 (2020) 325–337.

[40] M. Sefi, I.B. Amara, A. Troudi, N. Soudani, A. Hakim, K.M. Zeghal, et al., Effect of selenium on methimazole-induced liver damage and oxidative stress in adult rats and their offspring, Toxicol. Ind. Health 30 (2014) 653–669.

[41] M. Cengiz, S. Cetik Yildiz, C. Demir, İ.K. Şahin, Ö. Teksoy, A. Ayhanci, Hepato-preventive and anti-apoptotic role of boric acid against liver injury induced by cyclophosphamide, J. Trace Elem. Med. Biol. 53 (2019) 1–7.

[42] Cengiz M, Yeşildağ Ö, Ayhancı A. Siklofosfamid nedenli hematoksiste üzerine karvakrolün sitoprotektif etkileri. Türkiye Tarımsal Araştırmalar Dergisi.5:125-130.

[43] G.A. Raza, A. Ghaffar, R. Hussain, A. Jamal, Z. Ahmad, B.B. Mohamed, A.S. Aljohani, Nuclear and morphological alterations in erythrocytes, antioxidant enzymes, and genetic disparities induced by brackish water in mrigal carp (Cirrhinus mrigala), Oxid. Med. Cell. Longev. 2022 (2022) 4972622.

[44] M. Ahmad, A. Ghaffar, R. Hussain, R.U. Khan, Pymetrozine causes physical, haematological, blood biochemical and histopathological abnormalities in bighead carp (Aristichthys nobilis), Pakistan J. Zool. 55 (2023) 1575.

[45] X. Li, S. Naseem, R. Hussain, A. Ghaffar, K. Li, A. Khan, Evaluation of DNA damage, biomarkers of oxidative stress, and status of antioxidant enzymes in freshwater fish (Labeo rohita) exposed to pyriproxyfen, Oxid. Med. Cell. Longev. 2022 (2022) 5859266.

[46] Y. Mahmood, R. Hussain, A. Ghaffar, F. Ali, S. Nawaz, K. Mehmood, A. Khan, Acetochlor affects bighead carp (Aristichthys nobilis) by producing oxidative stress, lowering tissue proteins, and inducing genotoxicity, BioMed Res. Int. 2022 (2022) 9140060.

[47] J-q Wang, R. Hussain, A. Ghaffar, G. Afzal, A.Q. Saad, N. Ahmad, et al., Clinicohematological, mutagenic, and oxidative stress induced by pendimethalin in freshwater fish bighead carp (Hypophthalmichthys nobilis), Oxid. Med. Cell. Longev. 2022 (2022) 2093822.

[48] S. Naseem, A. Ghaffar, R. Hussain, A. Khan, Inquisition of toxic effects of pyriproxyfen on physical, hemato-biochemical and histopathological parameters in Labeo rohita fish, Pakistan Vet. J. 42 (2022).

[49] R. Hussain, A. Ghaffar, G. Abbas, G. Jabeen, I. Khan, R.Z. Abbas, et al., Thiamethoxam at sublethal concentrations induces histopathological, serum biochemical alterations and DNA damage in fish (Labeo rohita), Toxin Rev. 41 (2022) 154–164.

[50] A. Ali, S. Saeed, R. Hussain, M.S. Saif, M. Waqas, I. Asghar, et al., Exploring the impact of silica and silica-based nanoparticles on serological parameters, histopathology, organ toxicity, and genotoxicity in Rattus norvegicus, Applied Surface Science Advances 19 (2024) 100551.

[51] Y. Mahmood, A. Ghaffar, R. Hussain, New insights into hemato-biochemical and histopathological effects of acetochlor in bighead carp (Aristichthys nobilis), Pak. Vet. J. 41 (2021).

[52] R. Akram, R. Iqbal, R. Hussain, M. Ali, Effects of bisphenol a on hematological, serum biochemical, and histopathological biomarkers in bighead carp (Aristichthys nobilis) under long-term exposure, Environ. Sci. Pollut. Control Ser. (2021) 1–16.

[53] G. Afzal, H.I. Ahmad, R. Hussain, A. Jamal, S. Kiran, T. Hussain, et al., Bisphenol A induces histopathological, hematobiochemical alterations, oxidative stress, and genotoxicity in common carp (Cyprinus carpio L.), Oxid. Med. Cell. Longev. 2022 (2022) 5450421.

[54] G. Jabeen, F. Manzoor, M. Arshad, B. Barbol, Effect of cadmium exposure on hematological, nuclear and morphological alterations in erythrocyte of fresh water fish (Labeo rohita), Continental veterinary journal 1 (2021) 20–24.

[55] M. Namratha, M. Lakshman, M. Jeevanalatha, B. Kumar, Hematological alterations induced by glyphosate and ameliorative effect of ascorbic acid in Wistar rats, Continental Veterinary Journal 1 (2020) 32–36.

[56] H. Kiran, S. Kousar, F. Ambreen, R. Ilyas, S. Abbas, Effect of plant-based feed on the antioxidant enzymes, biochemical and hematological parameters of Oreochromis niloticus, Cont Vet J 2 (2022) 67–75.

[57] R. Akram, R. Iqbal, R. Hussain, F. Jabeen, M. Ali, Evaluation of oxidative stress, antioxidant enzymes and genotoxic potential of bisphenol A in fresh water bighead carp (Aristichthys nobils) fish at low concentrations, Environ. Pollut. 268 (2021) 115896.

[58] R. Hussain, F. Ali, M.T. Javed, G. Jabeen, A. Ghaffar, I. Khan, et al., Clinico-hematological, serum biochemical, genotoxic and histopathological effects of trichlorfon in adult cockerels, Toxin Rev. 40 (2021) 1206–1214.

[59] R. Hussain, F. Mahmood, M.Z. Khan, A. Khan, F. Muhammad, Pathological and genotoxic effects of atrazine in male Japanese quail (Coturnix japonica), Ecotoxicology 20 (2011) 1–8.

[60] D. Sun, C. Sun, G. Qiu, L. Yao, J. Yu, Sberi H. Al, et al., Allicin mitigates hepatic injury following cyclophosphamide administration via activation of Nrf2/ARE pathways and through inhibition of inflammatory and apoptotic machinery, Environ. Sci. Pollut. Control Ser. 28 (2021) 39625–39636.

[61] A. Iqubal, M.A. Syed, J. Ali, A.K. Najmi, M.M. Haque, S.E. Haque, Nerolidol protects the liver against cyclophosphamide-induced hepatic inflammation, apoptosis, and fibrosis via modulation of Nrf2, NF-κB p65, and caspase-3 signaling molecules in Swiss albino mice, Biofactors 46 (2020) 963–973.

[62] F. Sioud, I. Ben Toumia, A. Lahmer, R. Khlifi, Z. Dhaouefi, M. Maatouk, et al., Methanolic extract of Ephedra alata ameliorates cisplatin-induced nephrotoxicity and hepatotoxicity through reducing oxidative stress and genotoxicity, Environ. Sci. Pollut. Control Ser. 27 (2020) 12792–12801.

[63] B.E. Aboulhoda, D.A. Abdeltawab, L.A. Rashed, M.F. Abd Alla, H.D. Yassa, Hepatotoxic effect of oral zinc oxide nanoparticles and the ameliorating role of selenium in rats: a histological, immunohistochemical and molecular study, Tissue Cell 67 (2020) 101441.

[64] S. Gunes, V. Sahinturk, S. Uslu, A. Ayhanci, S. Kacar, R. Uyar, Protective effects of selenium on cyclophosphamide-induced oxidative stress and kidney injury, Biol. Trace Elem. Res. 185 (2018) 116–123.

[65] S. Ince, I. Kucukkurt, H.H. Demirel, D.A. Acaroz, E. Akbel, I.H. Cigerci, Protective effects of boron on cyclophosphamide induced lipid peroxidation and genotoxicity in rats, Chemosphere 108 (2014) 197–204.

[66] N.M. Mesalam, M.A. Ibrahim, M.R. Mousa, N.M. Said, Selenium and vitamin E ameliorate lead acetate-induced hepatotoxicity in rats via suppression of oxidative stress, mRNA of heat shock proteins, and NF-kB production, J. Trace Elem. Med. Biol. 79 (2023) 127256.

[67] A.M. Mahmoud, M.O. Germoush, M.F. Alotaibi, O.E. Hussein, Possible involvement of Nrf2 and PPARγ up-regulation in the protective effect of umbelliferone against cyclophosphamide-induced hepatotoxicity, Biomed. Pharmacother. 86 (2017) 297–306.

[68] E. Kar, F. Kar, B. Can, A. Çakır Gündoğdu, C. Özbayer, F.E. Koçak, H. Şentürk, Prophylactic and therapeutic efficacy of boric acid on lipopolysaccharide-induced liver and kidney inflammation in rats, Biol. Trace Elem. Res. 202 (2024) 3701–3713.

[69] R.M. Malyar, E. Naseri, H. Li, I. Ali, R.A. Farid, D. Liu, et al., Hepatoprotective effects of selenium-enriched probiotics supplementation on heat-stressed wistar rat through anti-inflammatory and antioxidant effects, Biol. Trace Elem. Res. 199 (2021) 3445–3456.

[70] G.Ö. Önder, Ö. Göktepe, O. Eda, Ö.C. Mat, D. Bolat, E. Balcioğlu, Y. Arzu, Boric acid ameliorates liver injury in rat induced by cyclophosphamide, Sakarya Tıp Dergisi 13 (2023) 210–216.

[71] T. Zhu, C. Zhang, J. Ren, Y. Cheng, Z. Gao, Y. Ji, et al., Antioxidative effect of wheat-grain moxibustion on cyclophosphamide-induced liver injury in mice based on Nrf2-Keap1 signaling pathway, Zhongguo Zhen jiu= Chinese Acupuncture & Moxibustion 44 (2024) 549–554.

[72] H. Hao, Y. Xu, R. Chen, S. Qi, X. Liu, B. Lin, et al., Protective effects of chlorogenic acid against cyclophosphamide induced liver injury in mice, Biotech. Histochem. 99 (2024) 33–43.

[73] C. Caglayan, Y. Temel, F.M. Kandemir, S. Yildirim, S. Kucukler, Naringin protects against cyclophosphamide-induced hepatotoxicity and nephrotoxicity through modulation of oxidative stress, inflammation, apoptosis, autophagy, and DNA damage, Environ. Sci. Pollut. Control Ser. 25 (2018) 20968–20984.

[74] A. Akcay, Q. Nguyen, C.L. Edelstein, Mediators of inflammation in acute kidney injury, Mediat. Inflamm. 2009 (2009).

[75] W. Gao, Z. Feng, S. Zhang, B. Wu, X. Geng, G. Fan, et al., Anti-inflammatory and antioxidant effect of Eucommia ulmoides polysaccharide in hepatic ischemia-reperfusion injury by regulating ROS and the TLR-4-NF-κB pathway, BioMed Res. Int. 2020 (2020) 1860637.

[76] D.H. Sami, A.S. Soliman, A.A. Khowailed, E.H.M. Hassanein, E.M. Kamel, A.M. Mahmoud, 7-hydroxycoumarin modulates Nrf2/HO-1 and microRNA-34a/SIRT1 signaling and prevents cisplatin-induced oxidative stress, inflammation, and kidney injury in rats, Life Sci. 310 (2022) 121104.

[77] A.M. Mahmoud, Dera HS. Al, 18β-Glycyrrhetinic acid exerts protective effects against cyclophosphamide-induced hepatotoxicity: potential role of PPARγ and Nrf2 upregulation, Genes & nutrition 10 (2015) 1–13.

[78] E.M. Kamel, A.M. Mahmoud, S.A. Ahmed, A.M. Lamsabhi, A phytochemical and computational study on flavonoids isolated from Trifolium resupinatum L. and their novel hepatoprotective activity, Food Funct. 7 (2016) 2094–2106.

[79] M.O. Germoush, A.M. Mahmoud, Berberine mitigates cyclophosphamide-induced hepatotoxicity by modulating antioxidant status and inflammatory cytokines, J. Cancer Res. Clin. Oncol. 140 (2014) 1103–1109.

[80] A. Iqubal, M.A. Syed, M.M. Haque, A.K. Najmi, J. Ali, S.E. Haque, Effect of nerolidol on cyclophosphamide-induced bone marrow and hematologic toxicity in Swiss albino mice, Exp. Hematol. 82 (2020) 24–32.

[81] F. Gür, M. Cengiz, B. Gür, O. Cengiz, O. Sarıçiçek, A. Ayhancı, Therapeutic role of boron on acrylamide-induced nephrotoxicity, cardiotoxicity, neurotoxicity, and testicular toxicity in rats: effects on Nrf2/Keap-1 signaling pathway and oxidative stress, J. Trace Elem. Med. Biol. (2023) 127274.

[82] S. Alqahtani, A.M. Mahmoud, Gamma-Glutamylcysteine ethyl Ester protects against cyclophosphamide-induced liver injury and hematologic alterations via upregulation of PPARγ and attenuation of oxidative stress, inflammation, and apoptosis, Oxid. Med. Cell. Longev. (2016) 2016.

[83] V. Pelmenschikov, P.E.M. Siegbahn, Copper−Zinc superoxide dismutase: theoretical insights into the catalytic mechanism, Inorg. Chem. 44 (2005) 3311–3320.

[84] T. Ramasarma, D. Vaigundan, Pathways of electron transfer and proton translocation in the action of superoxide dismutase dimer, Biochem. Biophys. Res. Commun. 514 (2019) 772–776.

[85] L.M. Amzel, Loss of translational entropy in binding, folding, and catalysis, Proteins: Struct., Funct., Bioinf. 28 (1997) 144–149.

[86] F. Gür, B. Gür, B. Erkayman, Z. Halıcı, A. Karakoç, Investigation of serum and brain superoxide dismutase levels depending on atomoxetine used in attention-deficit/hyperactivity disorder treatment: a combination of in vivo and molecular docking studies, Bioorg. Chem. 105 (2020) 104435.

[87] Y. Oğul, F. Gür, M. Cengiz, B. Gür, R.A. Sarı, A. Kızıltunç, Evaluation of oxidant and intracellular anti-oxidant activity in rheumatoid arthritis patients: in vivo and in silico studies, Int. Immunopharm. 97 (2021) 107654.

[88] M. Jing, G. Han, J. Wan, S. Zhang, J. Yang, W. Zong, et al., Catalase and superoxide dismutase response and the underlying molecular mechanism for naphthalene, Sci. Total Environ. 736 (2020) 139567.

[89] K. Kavanagh, C. Johansson, C. Smee, O. Gileadi, F. Von Delft, J. Weigelt, et al., Crystal structure of the selenocysteine to glycine mutant of human glutathione peroxidase 1, The Research Collaboratory for Structural Bioinformatics (RCSB) RCSB-Rutgers (2010).

[90] J.L. Janetzki, N.L. Pratt, M.B. Ward, M.J. Sykes, Application of an integrative drug safety model for detection of adverse drug events associated with inhibition of glutathione peroxidase 1 in chronic obstructive pulmonary disease, Pharmaceut. Res. 40 (2023) 1553–1568.